






Article

New Diarylamine K_V10.1 Inhibitors and Their Anticancer Potential

Špela Gubič¹ , Žan Toplak¹ , Xiaoyi Shi², Jaka Dernovšek¹, Louise Antonia Hendrickx³, Ernesto Lopes Pinheiro-Junior³ , Steve Peigneur³ , Jan Tytgat³, Luis A. Pardo² , Lucija Peterlin Mašič¹  and Tihomir Tomašič^{1,*} 

¹ Faculty of Pharmacy, University of Ljubljana, Aškerčeva cesta 7, 1000 Ljubljana, Slovenia

² AG Oncophysiology, Max-Planck Institute for Experimental Medicine, Hermann-Rein-Str. 3, 37075 Göttingen, Germany

³ Toxicology and Pharmacology, Campus Gasthuisberg, University of Leuven, Onderwijs en Navorsing 2, Herestraat 49, 3000 Leuven, Belgium

* Correspondence: tihomir.tomasich@ffa.uni-lj.si

Abstract: Expression of the voltage-gated potassium channel K_V10.1 (Eag1) has been detected in over 70% of human cancers, making the channel a promising new target for new anticancer drug discovery. A new structural class of K_V10.1 inhibitors was prepared by structural optimisation and exploration of the structure–activity relationship of the previously published hit compound ZVS-08 (**1**) and its optimised analogue **2**. The potency and selectivity of the new inhibitors between K_V10.1 and hERG were investigated using whole-cell patch-clamp experiments. We obtained two new optimised K_V10.1 inhibitors, **17a** and **18b**, with improved nanomolar IC₅₀ values of 568 nM and 214 nM, respectively. Compound **17a** exhibited better ratio between IC₅₀ values for hEAG1 and hERG than previously published diarylamine inhibitors. Compounds **17a** and **18b** moderately inhibited the growth of the K_V10.1-expressing cell line MCF-7 in two independent assays. In addition, **17a** and **18b** also inhibited the growth of hERG-expressing Panc-1 cells with higher potency compared with MCF-7 cells. The main obstacle for newly developed diarylamine K_V10.1 inhibitors remains the selectivity toward the hERG channel, which needs to be addressed with targeted drug design strategies in the future.

Keywords: K_V10.1; ion channels; hERG; SAR; antiproliferative activity



Citation: Gubič, Š.; Toplak, Ž.; Shi, X.; Dernovšek, J.; Hendrickx, L.A.; Pinheiro-Junior, E.L.; Peigneur, S.; Tytgat, J.; Pardo, L.A.; Mašič, L.P.; et al. New Diarylamine K_V10.1 Inhibitors and Their Anticancer Potential. *Pharmaceutics* **2022**, *14*, 1963. <https://doi.org/10.3390/pharmaceutics14091963>

Academic Editors: Noelia Duarte and Ana Paula Francisco

Received: 23 August 2022

Accepted: 14 September 2022

Published: 17 September 2022

Publisher's Note: MDPI stays neutral with regard to jurisdictional claims in published maps and institutional affiliations.



Copyright: © 2022 by the authors. Licensee MDPI, Basel, Switzerland. This article is an open access article distributed under the terms and conditions of the Creative Commons Attribution (CC BY) license (<https://creativecommons.org/licenses/by/4.0/>).

1. Introduction

The voltage-gated potassium channel K_V10.1 (Eag1) is one of the eight members of the ether-à-go-go family, which is itself subdivided into three subfamilies (Eag, Erg, and Elk) [1,2]. Analogous to other K_V channels, Eag1 is formed by four subunits, with each monomer consisting of six transmembrane segments (S1–S6). The voltage-sensor domain (VSD), which consists of segments S1–S4, detects changes in membrane potential and triggers conformational changes, leading to pore opening. Segments S5 and S6 (pore domain, PD) of each monomer join together to form the ion-conducting pore, which includes the water-filled cavity and the selectivity filter (SF). The second part represents the narrowest part of the pore, which is lined with oxygen atoms that coordinate the movement of potassium ions during permeation [3].

The channel K_V10.1 has emerged as a very attractive oncological target in the last two decades. The channel is mainly expressed in healthy tissues of the central nervous system, while it is barely detectable in peripheral tissues, with the exception of testis and adrenal gland [4,5]. Aberrant K_V10.1 expression has been detected in over 70% of human cancers, regardless of tumour type, which is why the channel is considered a nearly universal tumour marker [6]. K_V10.1 activity is involved in important processes for cancer cell growth and spread, such as cell cycle control, proliferation, migration, angiogenesis, and resistance to hypoxia [7]. The mechanisms of the channel's involvement in cancer proliferation appear to be related to alterations in membrane potential control and non-canonical effects of

overexpressed $K_V10.1$, affecting Ca^{2+} signalling and microtubule dynamics [8]. Previous *in vitro* and *in vivo* studies have shown that specific inhibition of $K_V10.1$ can successfully reduce tumour progression [9–13]. On this basis, the channel is a promising target for new anticancer drug discovery. Novel selective $K_V10.1$ inhibitors could, therefore, prolong the survival of patients with fibrosarcoma [14], ovarian cancer [15], glioblastoma [16], acute lymphoid leukaemia [17], gastric [18], head and neck [19], and colon cancer [20], in which the expression of the channel is significantly higher than in normal tissues. Moreover, in a retrospective study, $K_V10.1$ inhibitors have already shown an effective improvement in survival in a group of patients with brain metastases compared to an untreated control group [16]. To date, no specific and selective small-molecule $K_V10.1$ inhibitors have been reported because they all exhibited significant inhibition of the cardiac hERG channel, which raised major concerns about adverse cardiac side effects [21]. Recent studies have pointed to a particular structural difference between $K_V10.1$ and hERG channels that has profound functional implications and suggests the possibility of selective inhibition of $K_V10.1$ in cancer therapies [22].

To date, only a very small number of compounds has been described to act on $K_V10.1$ [21]. Most small molecules were identified by studying $K_V10.1$ inhibition of the previously described antitumour agents and hERG inhibitors, as these channels share structural similarities. $K_V10.1$ inhibitors can interact with the channel at multiple binding sites, including VSD and PD. Since $K_V10.1$ and hERG share a high structural similarity in the central cavities, designing a selective small molecule that blocks the pore is a major challenge [23]. In contrast, a more promising approach is to target the VSD domain. Small molecules, such as mibefradil, purpurealidin I analogues, amiodarone, and 20(*S*)-ginsenoside Rg3 (Figure 1), bind to VSD and act as gating modifiers [24,25]. The exact binding sites of these inhibitors are not yet known, but new cryo-electron microscopy structures of $K_V10.1$ and hERG may contribute to the development of new specific inhibitors that bind to VSD [3,23].

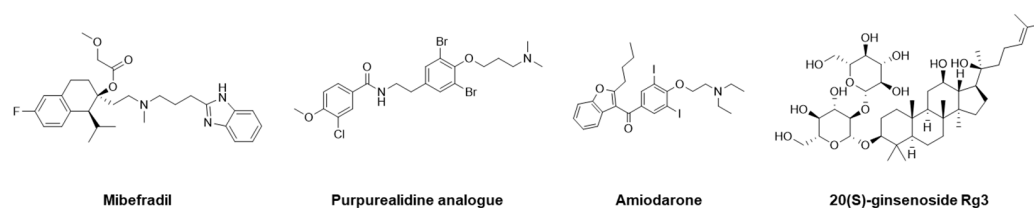


Figure 1. Structures of known ligands binding to the voltage-sensor domain of $K_V10.1$.

Our research group recently published a novel structural class of $K_V10.1$ inhibitors discovered by a unique ligand-based drug design strategy [26]. Compound ZVS-08 (**1**, Figure 2) with a diarylamine structure was identified as a hit compound in a computational 3D pharmacophore model. In biological assays, it inhibited the $K_V10.1$ channel with the effect of the gating modifier ($IC_{50} = 3.70 \mu M$). The even more potent $K_V10.1$ inhibitor **2** ($IC_{50} = 740 \text{ nM}$, Figure 2) was obtained by structure–activity relationship studies. Compound **2** was appropriately selective for some K_V and Na_V channels, but also showed significant hERG inhibition ($IC_{50} = 207 \text{ nM}$). Growth of the breast cancer cell line MCF-7, which has high $K_V10.1$ levels and low hERG levels, was more strongly inhibited by compound **2** than the growth of Panc-1 cells, which have low $K_V10.1$ levels and high hERG levels. Compound **2** also induced significant apoptosis in tumour spheroids of Colo357 cells. Here, we present a new series of potent nanomolar $K_V10.1$ inhibitors obtained by structural optimisation of previously published compounds **1** and **2**. We also demonstrated the potential of this new structural class of $K_V10.1$ inhibitors for antiproliferative activity in MCF-7 cancer cell models.

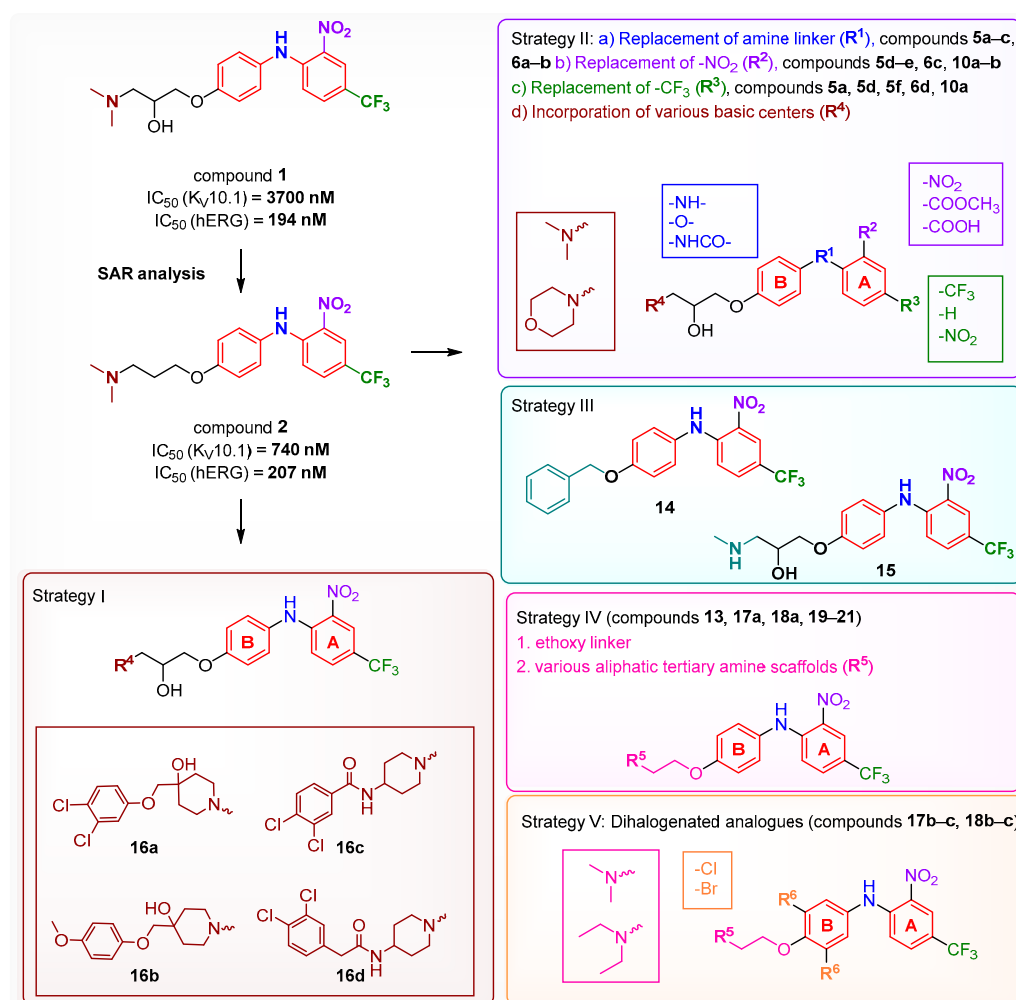


Figure 2. Design of the hit compound ZVS-08 (1) analogues (Strategies I–V).

2. Materials and Methods

2.1. Synthetic Procedures and Analytical Data

Reagents and solvents for the syntheses were from Fluorochem Ltd. (Derbyshire, UK), Apollo Scientific Ltd. (Stockport, UK), Sigma-Aldrich (St. Louis, MO, USA), Enamine Ltd. (Kiev, Ukraine), and TCI (Tokyo, Japan), and were not further purified. Analytical thin-layer chromatography was performed on silica gel aluminium plates (0.20 mm; 60 F254; Merck, Darmstadt, Germany). Silica gel 60 (particle size 230–400 mesh) was used for column chromatography. Reversed-phase column chromatography (RP-CC) was performed on the Isolera Biotage One Flash Chromatography system (SNAP Biotage KP-C18-HS column, 12 g, Biotage, Uppsala, Sweden) using a gradient of 0.1% TFA in deionised water and MeCN as eluent (gradient 10–100% MeCN in 15 column volumes (300 mL); 100% MeCN for 5 column volumes (100 mL)). ^1H and ^{13}C NMR spectra were recorded using a 400 MHz NMR spectrometer (Bruker Advance 3, Bruker, Billerica, MA, USA). The splitting patterns were designated as follows: s, singlet; d, doublet; dd, double doublet; td, triple doublet; t, triplet; dt, double triplet; ddd, double of doublet of doublet; ddt, doublet of doublet of triplets; q, quartet; and m, multiplet. The purity of the prepared compounds was verified by liquid chromatography-mass spectrometry according to method A (see below) on a Thermo Scientific Dionex UltiMate 3000 modular system (Thermo Fisher Scientific Inc., Waltham, MA, USA). HRMS measurements were performed on an LC-MS/MS system (Exactive Plus Orbitrap mass spectrometer; Thermo Scientific Inc., Waltham, MA, USA). The high-resolution mass spectra (HRMS) used optical rotation detection at $\lambda = 589 \text{ nm}$ (Polarimeter model 241; Perkin Elmer, Boston, MA, USA).

Analytical reversed-phase UPLC analyses were performed using a modular system (Thermo Scientific Dionex UltiMate 3000 modular system; Thermo Fisher Scientific Inc., MA, USA). Method: Waters Acquity UPLC[®] HSS C18 SB column (2.1 × 50 mm, 1.8 μm), T = 40 °C; injection volume = 5 μL; flow rate = 0.4 mL/min; detector λ = 254 nm; mobile phase A (0.1% TFA [*v/v*] in water), mobile phase B (MeCN). Gradient: 0–2 min, 10% B; 2–10 min, 10–90% B; 10–12 min, 90% B. The purity of the tested compounds was determined to be ≥95% by UPLC at 254 nm.

Detailed chemical synthesis procedures and chemical analysis results of all intermediates and final compounds **3a–b**, **4a–g**, **5a–f**, **6a–d**, **7**, **8a–b**, **9a–b**, **10a–b**, **11**, **12a–d**, **13**, **14**, **15**, **16a–d**, **17a–c**, **18a–c**, **19**, **20**, and **21** are described in Appendix A and Supplementary Materials.

2.2. Electrophysiological Recordings on HEK-293 Cells

For whole-cell patch-clamp measurements, stably transfected HEK-293 cells expressing K_V10.1 [26–28] were grown in DMEM with 10% FCS and 300 μg/mL Zeocin on glass coverslips coated with fibronectin. All experiments were conducted at room temperature under perfusion by gravity with extracellular solution (160 mM NaCl, 2.5 mM KCl, 2 mM CaCl₂, 1 mM MgCl₂, 10 mM Hepes pH 7.4 with NaOH, 8 mM glucose). Pipettes were made from #1 glass capillaries (WPI) and had 1–3 MΩ resistance. The intracellular solution contained 100 mM KCl, 45 mM *N*-methyl-D-glucamine, 10 mM 1,2-bis(*o*-aminophenoxy)ethane-*N,N,N',N'*-tetraacetic acid (BAPTA), 10 mM Hepes pH 7.35. Stimulation was applied and data were acquired with an EPC10 Plus amplifier (HEKA Elektronik) controlled with Patch Master software. Compounds were applied with an 8-channel fast solution exchanger (ALA). Compounds were prepared to a stock concentration of 10 mM in DMSO. The control solution contained 0.5% DMSO. Stimuli consisted of 500 ms depolarizations to +40 mV.

2.3. Electrophysiological Recordings on *Xenopus laevis* Oocytes

Stage V–VI oocytes were isolated by partial ovariectomy from *Xenopus laevis* frogs (African clawed frog) [26]. Mature female frogs were purchased from CRB Xénopes (Rennes, France) and were housed in the Aquatic Facility (KU Leuven) in compliance with the regulations of the European Union (EU) concerning the welfare of laboratory animals as declared in Directive 2010/63/EU. The use of *Xenopus laevis* was approved by the Animal Ethics Committee of the KU Leuven (Project nr. P186/2019). After anaesthetising the frogs by a 15 min submersion in 0.1% tricaine methanesulphonate (pH 7.0), the oocytes were collected. The isolated oocytes were then washed with a 1.5 mg/mL collagenase solution for 2 h to remove the follicle layer.

Ion channels (K_V10.1 and hERG) were expressed in *Xenopus laevis* oocytes, by linearisation of the plasmids and subsequent *in vitro* transcription using a commercial T7 or SP6 mMMESSAGE mMACHINE transcription kit (Ambion, Carlsbad, CA, USA). Defolliculated *Xenopus* oocytes were then injected with 20–50 nL of the cRNA at a concentration of 1 ng/nL using a micro-injector (Drummond Scientific1, Broomall, PA, USA). The oocytes were incubated in a solution containing (in mM): NaCl, 96; KCl, 2; CaCl₂, 1.8; MgCl₂, 2 and HEPES, 5 (pH 7.4), supplemented with 50 mg/L gentamycin sulphate and 90 mg theophylline. After *ex vivo* translation, the ion channels are correctly inserted in the cell membrane of the oocytes.

Two-electrode voltage-clamp recordings were performed at room temperature (18–22 °C) using a Geneclamp 500 amplifier (Molecular Devices, San Jose, CA, USA) controlled by a pClamp data acquisition system (Axon Instruments1, Union City, CA, USA) and using an integrated digital TEVC amplifier controlled by HiClamp, an automated Voltage-Clamp Screening System (Multi Channel Systems MCS GmbH, Reutlingen, Germany). Whole-cell currents from oocytes were recorded 1–7 days after injection. The bath solution composition was ND96 (in mM): NaCl, 96; KCl, 2; CaCl₂, 1.8; MgCl₂, 2 and HEPES, 5 (pH 7.5). Voltage and current electrodes were filled with a 3 M solution of KCl in H₂O. Resistances of both electrodes were kept between 0.5 and 1.5 MΩ. The elicited K_V10.1 and hERG currents were filtered at 0.5 kHz and sampled at 2 kHz using a four-pole low-pass Bessel filter.

Leak subtraction was performed using a p/4 protocol. Starting from a holding potential of -90 mV, currents for Kv10.1 were evoked by 1 s depolarizing pulses to 0 mV and currents for hERG were evoked by 2.5 s depolarizing prepulses to +40 mV, followed by hyperpolarizing pulses to -120 mV for 2.5 s. The concentration dependency of all compounds was assessed by measuring the current inhibition in the presence of increasing compound concentrations. To this end, a stock solution of the compounds was prepared in 100% DMSO for the sake of solubility. From this stock solution, adequate dilutions with a maximum of 0.5% DMSO were made for testing. The data of the concentration–response curves were fitted with the Hill equation: $y = 100 / \{1 + (IC_{50} / [\text{compound}])^h\}$, where y is the amplitude of the compound-induced effect, IC_{50} is the compound concentration at half-maximal efficacy, (compound) is the compound concentration, and h is the Hill coefficient.

2.4. Statistical Analysis

All electrophysiological data are presented as means \pm SEM of $n \geq 3$ independent experiments unless otherwise indicated. Oocyte data were analysed using pClamp Clampfit 10.4 (Molecular Devices, Downingtown, PA, USA) and OriginPro 9 (Originlab, Northampton, MA, USA) or GraphPad Prism 8 software (GraphPad Software, Inc., San Diego, CA, USA). Patch-clamp data analysis was performed using FitMaster (HEKA Electronics), IgorPro (Wavemetrics, Inc., Lake Oswego, OR, USA) and GraphPad Prism 9 (GraphPad Software, Inc., San Diego, CA, USA). The Dunnett test and one-way ANOVA were performed to calculate the significance of the induced inhibition compared to the control ($p < 0.05$).

2.5. Cell Culture

MCF-7 (DSMZ ACC 115) and PANC-1 (DSMZ ACC 783) cells were grown as recommended by the cell supplier at 5% CO_2 and 37 °C in a humidified atmosphere. For determining cell growth, cells were seeded in 96-well culture plates (Corning, Corning, NY, USA) at a density of 10^4 cells/well. After 24 h, the compounds were added diluted in medium. Six wells per condition were used. Four images of each well were collected at 1 h intervals for 48–72 h. Two biological replicates were performed. Images were acquired using an Incucyte device (Sartorius/Essex biosciences). Cell confluence was calculated using the Incucyte software on the phase contrast images. The results are expressed as percent confluence per well normalised to the value with no compounds added.

2.6. MTS Assay

The antiproliferative activities of the compounds were evaluated on the breast cancer cell line MCF-7 (ATCC HTB-22, adherent cells isolated from a 69-year-old white woman), using an MTS (Promega, Madison, WI, USA) assay according to the manufacturer's instructions [29]. The MCF-7 cell line was obtained from the American Type Culture Collection (ATCC, Manassas, VA, USA). Cells were cultured in low-glucose Dulbecco's Modified Eagle's Medium (DMEM) (Sigma-Aldrich, St. Louis, MO, USA), supplemented with 10% fetal bovine serum (Gibco, Thermo Fisher Scientific, Waltham, MA, USA), 100 U/mL penicillin (Sigma-Aldrich, St. Louis, MO, USA), 100 μ g/mL streptomycin (Sigma-Aldrich, St. Louis, MO, USA), and 2 mM L-glutamine (Sigma-Aldrich, St. Louis, MO, USA). The cell line was incubated in a 5% CO_2 atmosphere at 37 °C. Cells were plated out in 96-well plates at a density of 2000 cells per well and incubated overnight. The next day, cells were treated with the indicated compounds, positive control (17-DMAG), or vehicle control (0.5% DMSO) and incubated for 72 h. Then CellTiter96 Aqueous One Solution Reagent (10 μ L; Promega, Madison, WI, USA) was added to each well and cells were incubated for an additional 3 h. Absorbance was measured at 492 nm using a microplate reader (Synergy 4 Hybrid; BioTek, Winooski, VT, USA). Independent experiments were repeated twice, each time in triplicate. Statistical significance ($p < 0.05$) was calculated using a two-tailed Welch's t -test between treated groups and DMSO. IC_{50} values are given as averages of the independent measurements and were calculated using GraphPad Prism 8.0 software (San

Diego, CA, USA). IC₅₀ values represent the concentration at which a compound elicits a half-maximal response.

3. Results

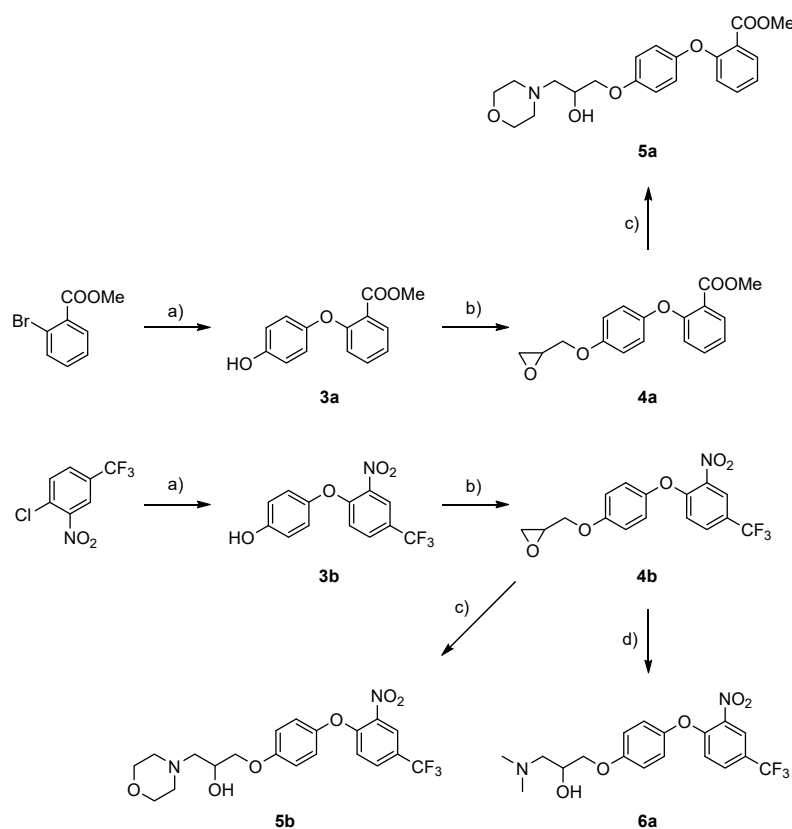
3.1. Design

New K_V10.1 inhibitors were designed and synthesised to increase the potency of published compounds **1** (ZVS-08) and **2** against K_V10.1 and selectivity against hERG, and to investigate structure–activity relationships (SAR) important for K_V10.1 inhibition. Compound **1** (Figure 2) with diarylamine structure and 1-(dimethylamino)-propan-2-ol segment attached to aromatic moiety B was modified in the different parts (R¹–R⁶) of the molecule to obtain a focused library of compounds screened for K_V10.1 inhibition (Figure 2, strategies I–V). In strategy I, the basic dimethylamino centre of ZVS-08 (**1**) was extended to different cyclic amines bearing aromatic rings (R⁴, Figure 2) to obtain new analogues with three aromatic scaffolds. The aim of strategy II (Figure 2) was to investigate the importance of the amine linker (R¹) and the electron-withdrawing nitro (R²) and trifluoromethyl (R³) groups of the hit compound ZVS-08 (**1**) and compound **2** for K_V10.1 inhibition. As a result, several new analogues with modifications at four different positions (R¹–R⁴) were developed. The new analogues in strategy II contained the cationic dimethylamino centre of hit compound **1** or was replaced by a morpholino group (R⁴) to maintain the basic character of the compound but further increase its polarity. Using strategy III (Figure 2), we tested whether the basic dimethylamino centre was required for the inhibition of K_V10.1. Therefore, two new analogues with modifications of this segment were developed. Since the hydroxyl group of ZVS-08 (**1**) was found not to be an important structural component for the inhibition of K_V10.1 (based on the comparison between **1** and **2**, Figure 2), the new analogues of strategy IV contained different aliphatic tertiary amine basic centres connected to the aromatic part B via a shorter ethoxy linker. The new dihalogenated analogues (strategy V, Figure 2) contained additional chloride or bromide atoms in aromatic part B and dimethylamino- or diethylamino-ethoxy groups.

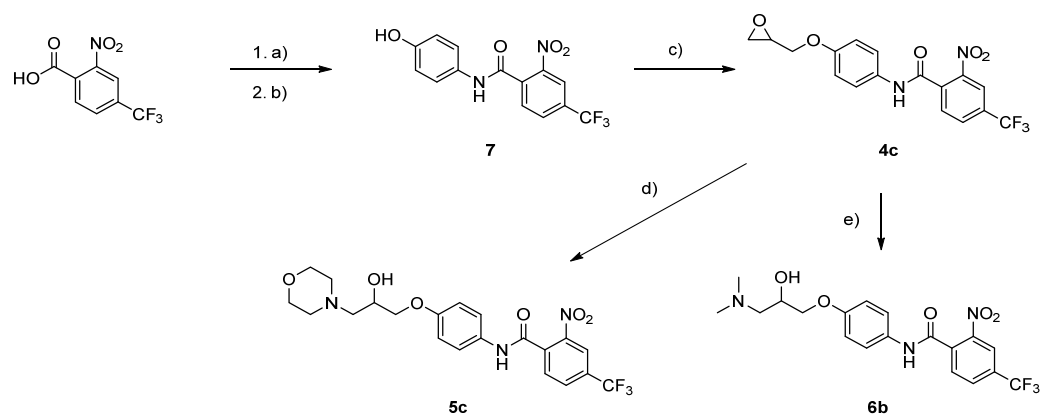
3.2. Synthesis

The syntheses of the new analogues are shown in Schemes 1–5. The differently substituted diarylphenols **3a–b**, **7**, **8a–b**, and **12a–d** were prepared through four different procedures. The synthesis of 4-hydroxyphenoxy analogues **3a–b** was carried out with the addition of CuO as a catalyst and a base at high temperature (Scheme 1) [30]. For the preparation of benzamide **7**, 2-nitro-4-(trifluoromethyl)benzoic acid was first converted with oxalyl chloride to the corresponding benzoyl chloride and the product was then refluxed in the presence of base and *p*-aminophenol to give benzamide **7** (Scheme 2). For the synthesis of compounds **8a–b** without the electron-withdrawing nitro group, CuO and Cu were used as catalysts (Scheme 3) [30]. The carboxylic acids **8a–b** were converted to the methyl esters **9a–b** by addition of thionyl chloride in anhydrous methanol (Scheme 3). *o*-Nitro-*p*-trifluoromethyl-substituted diarylphenols **12a** and **12c–d** were synthesised in two separate steps (Schemes 4 and 5). First, the nitro group was introduced by nitration of 1-chloro-4-(trifluoromethyl)benzene with concentrated nitric and sulfuric acids to give **11**, followed by the addition of the nonhalogenated or dihalogenated *p*-aminophenols at high temperature in the presence of a base to give **12a** and **12c–d** [31]. The dinitro-substituted compound **12b** was prepared by coupling *p*-aminophenol and 1-fluoro-2,4-dinitrobenzene with the addition of a base at reflux (Scheme 4). Epoxides **4a–g** were prepared using (±)-epichlorohydrin and K₂CO₃ as base (Schemes 1–4). For the epoxide opening, morpholine was used to give a racemic mixture of compounds **5a–f**, dimethylamine to give a racemic mixture of compounds **6a–d**, methylamine to give a racemic mixture of compound **15**, and the corresponding amines with aromatic moieties to give a racemic mixture of analogues **16a–d**. The methyl esters **5d** and **6c** were hydrolysed with 1 M sodium hydroxide to form the corresponding benzoic acids **10a–b** (Scheme 3). Compounds **13**, **19**, **20**, and **21** were prepared from *o*-nitro-*p*-trifluoromethyl-substituted diarylamine phe-

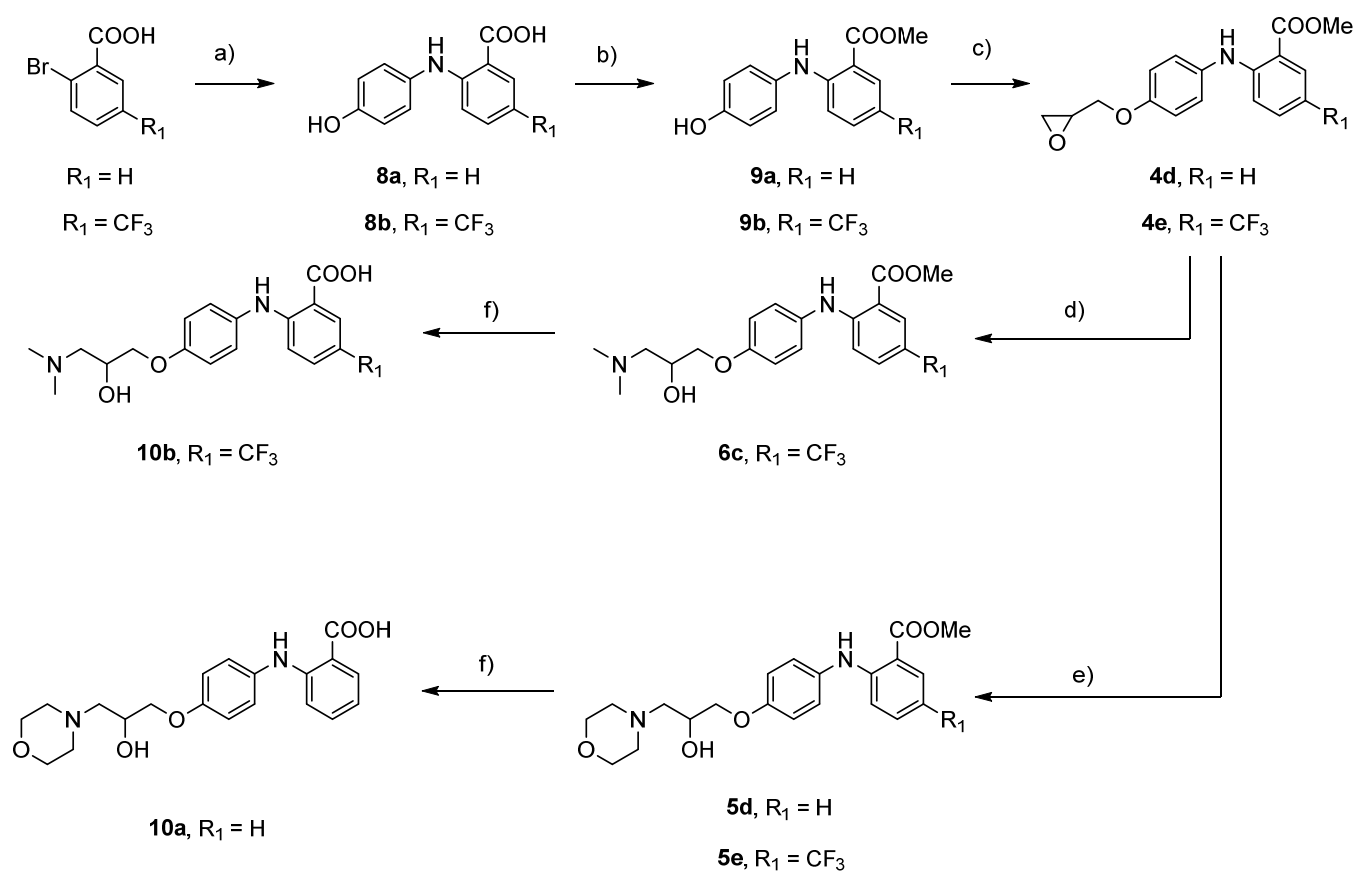
mol **12a** by addition of 4-(2-chloroethyl)morpholine for **13**, 1-(2-chloroethyl)pyrrolidine for **19**, 1-(2-chloroethyl)piperidine for **20**, or 1-(2-chloroethyl)azepane for **21** and base at reflux (Schemes 4 and 5). Compound **14** was synthesised from **12a** by addition of 4-benzyloxyaniline and base at high temperature (Scheme 4). Differently substituted diethylamino and dimethylamino analogues were formed at reflux from nonhalogenated or dihalogenated diarylamine phenols **12a** or **12c–d** by addition of base and 2-chloro-*N,N*-diethylethan-1-amine for **17a–c** or 2-chloro-*N,N*-dimethylethan-1-amine for **18a–c**.



Scheme 1. Reagents, solvents, and conditions: (a) hydroquinone, K_2CO_3 , CuO, pyridine, $110^\circ C$, 72 h; (b) (\pm) -epichlorohydrin, MeCN, K_2CO_3 , $80^\circ C$, 16 h; (c) morpholine, acetonitrile, r.t., 72 h; (d) $Me_2NH \times HCl$, K_2CO_3 , MeCN, $70^\circ C$, 24 h.



Scheme 2. Reagents, solvents, and conditions: (a) Oxalyl chloride, 2 drops of DMF, dichloromethane, $40^\circ C$, 24 h; (b) 4-aminophenol, triethylamine (TEA), MeCN, reflux, 24 h; (c) (\pm) -epichlorohydrin, MeCN, K_2CO_3 , $80^\circ C$, 16 h; (d) morpholine, MeCN, r.t., 72 h; (e) $Me_2NH \times HCl$, MeCN, K_2CO_3 , $70^\circ C$, 24 h.

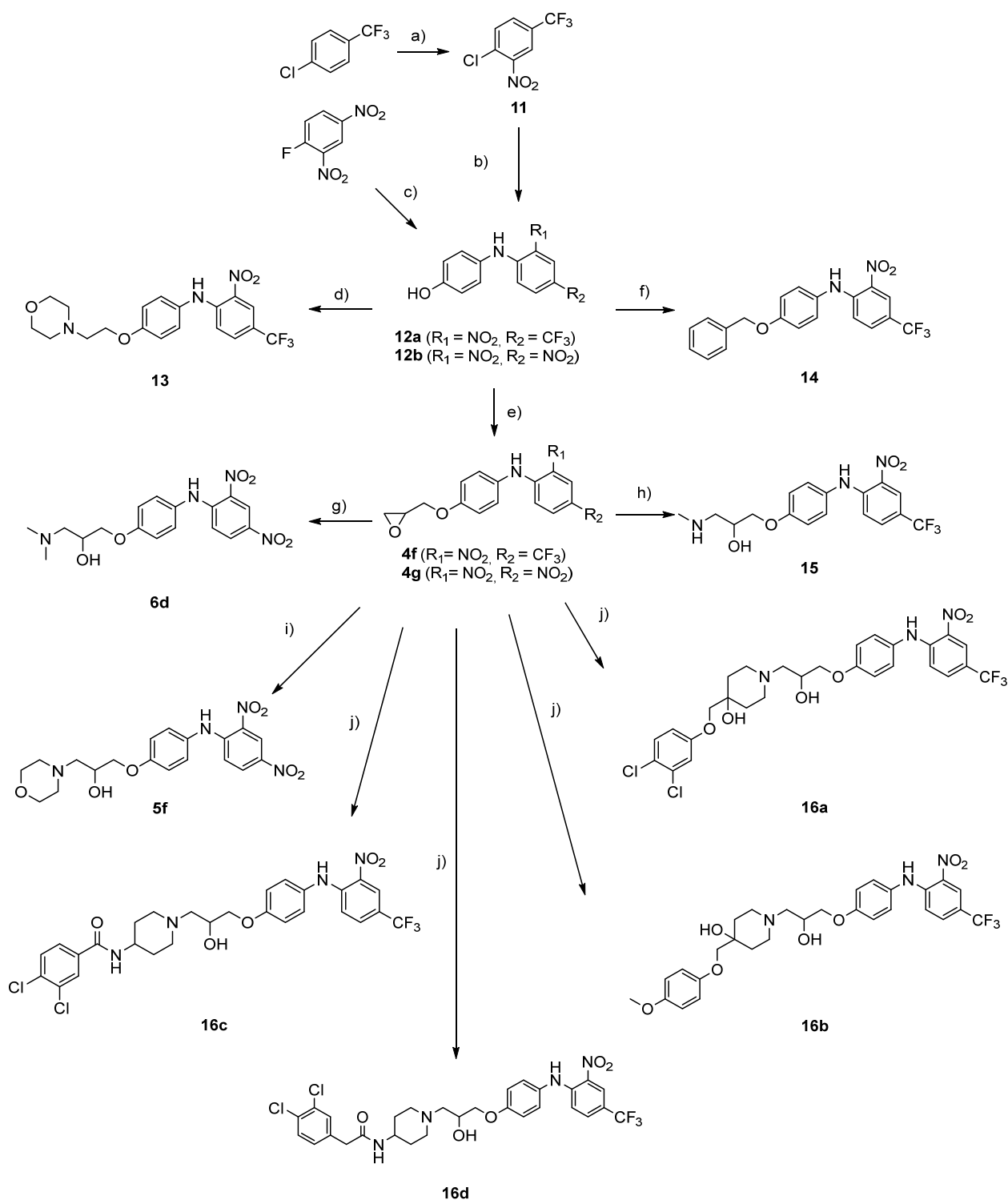


Scheme 3. Reagents, solvents, and conditions: (a) 4-aminophenol, K_2CO_3 , CuO, Cu, 2-ethoxyethanol, $130\text{ }^\circ\text{C}$, 16 h; (b) thionyl chloride, anhydrous MeOH, $70\text{ }^\circ\text{C}$, overnight; (c) (\pm)-epichlorohydrin, MeCN, K_2CO_3 , $80\text{ }^\circ\text{C}$, 16 h; (d) $Me_2NH \times HCl$, acetonitrile, K_2CO_3 , $70\text{ }^\circ\text{C}$, 24 h; (e) morpholine, dichloromethane, r.t., 72 h; (f) NaOH, EtOH, water, r.t., 72 h.

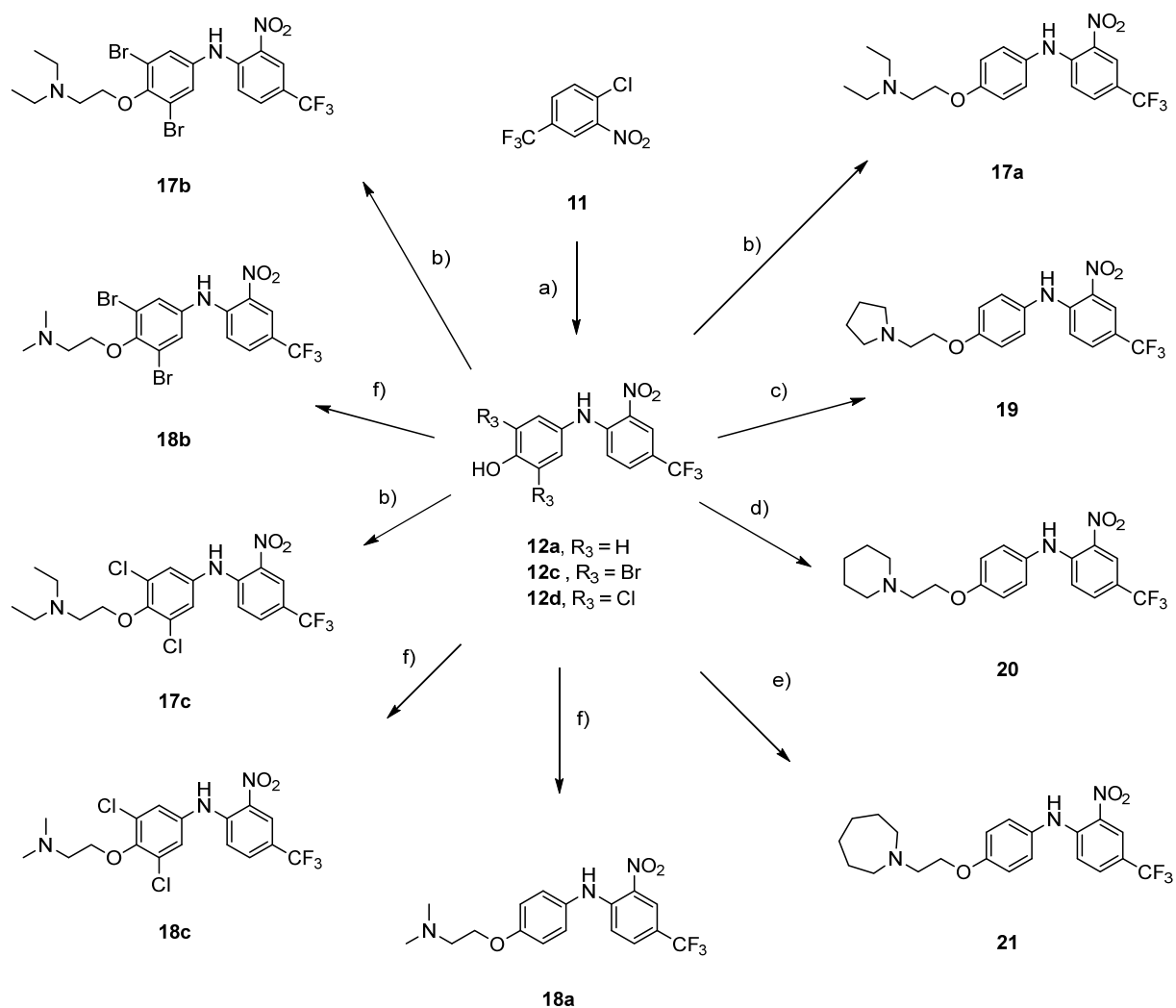
3.3. Analogues of Compounds 1 and 2 and Structure–Activity Relationships

Five different types of new $K_V10.1$ inhibitors were designed and synthesised to increase the potency on $K_V10.1$. Based on the study of the structure–activity relationships (SAR) of the analogues of ZVS-08 (**1**), we identified the structural components in this structural type of $K_V10.1$ inhibitor that are important for $K_V10.1$ inhibition.

The new analogues **16a–d**, based on three aromatic scaffolds (Table 1, strategy I), were an unsuccessful attempt to increase the potency of previously published compounds **1** and **2**. Similarly, almost all compounds from strategy II (Table 2) were inactive at $10\text{ }\mu\text{M}$ unless an amine linker (R^1), two nitro groups (R^2 and R^3), and morpholino (**5f**, R^4) or dimethylamino (**6d**, R^4) basic centres were present. Compound **14** from strategy III without a tertiary amine (R^4) was inactive as a $K_V10.1$ inhibitor (Table 3), but analogue **15** with a secondary aliphatic methylamine showed significant inhibition of the $K_V10.1$ current. Because the results for the new analogues of strategies II and III showed that the amine linker (R^1), two electron-withdrawing groups ($-NO_2$ as R^2 and $-CF_3$ as R^3), and the aliphatic tertiary amine (R^4) were very important structural elements for the inhibitory activity, these structural elements were included in the new compounds of strategies IV and V, but the alkoxy segments of **1** and **2** (strategies IV and V) and their second aromatic part (strategy V) were modified. The new compounds in strategy IV (Table 4), which included shorter ethoxy linkers and different aliphatic tertiary amines, such as diethylamine (**17a**), dimethylamine (**18a**), piperidin-1-yl (**20**) and azepan-1-yl (**21**) were the most potent $K_V10.1$ inhibitors. Some of the new dihalogenated diarylamines in strategy V (Table 5) with basic diethylamine or dimethylamine centres caused a high-percentage inhibition of $K_V10.1$ already at $1\text{ }\mu\text{M}$.



Scheme 4. Reagents, solvents, and conditions: (a) H₂SO₄, HNO₃, 80 °C, 1 week; (b) 4-aminophenol, NaHCO₃, MeCN, 90 °C, 24 h; (c) 4-aminophenol, NaHCO₃, MeCN, 90 °C, 24 h; (d) 4-(2-chloroethyl)morpholine, KOH, EtOH, 100 °C, overnight; (e) (±)-epichlorohydrin, MeCN, K₂CO₃, 80 °C, 16 h; (f) 4-benzyloxy aniline, NaHCO₃, toluene, 100 °C, 24 h; (g) Me₂NH × HCl, MeCN, 70 °C, 24 h; (h) MeNH₂, K₂CO₃, MeCN, 70 °C, 24 h; (i) morpholine, dichloromethane, r.t., 72 h; (j) appropriate amine, K₂CO₃, MeCN, 70 °C, 24 h.



Scheme 5. Reagents, solvents, and conditions: (a) 4-aminophenol or 4-amino-2,6-dibromophenol or 4-amino-2,6-dichlorophenol, NaHCO₃, MeCN, 90 °C, 24 h; (b) 2-chloro-*N,N*-diethylethan-1-amine × HCl, KOH or K₂CO₃, EtOH or MeCN, 100 °C or 90 °C, overnight; (c) 1-(2-chloroethyl)pyrrolidine × HCl, K₂CO₃, MeCN, 90 °C, 24 h; (d) 1-(2-chloroethyl)piperidine × HCl, K₂CO₃, MeCN, 90 °C, 24 h; (e) 1-(2-chloroethyl)azepane hydrochloride × HCl, K₂CO₃, MeCN, 90 °C, 24 h; (f) 2-chloro-*N,N*-dimethylethan-1-amine × HCl, MeCN, KOH or K₂CO₃, 100 °C or 90 °C, 16 h.

Table 1. Structures and potencies of compounds from Strategy I.

Strategy I		
Compound ID	R ⁴	% of Kv10.1 Inhibition at 50 μM (HEK-293 Cells)
16a		44.6 ± 8.6%
16b		60.7 ± 9.6%
16c		26.8 ± 10.1%
16d		21.8 ± 4.4%

Table 2. Structures and potencies of compounds from Strategy II.

Strategy II					
Compound ID	R ¹	R ²	R ³	R ⁴	% of Kv10.1 Inhibition at 10 μM (HEK-293 Cells)
5a	O	COOCH ₃	H		4.1 ± 2.6%
5b	O	NO ₂	CF ₃		2.9 ± 5.3%
5c	NHCO	NO ₂	CF ₃		7.5 ± 3.5%
5d	NH	COOCH ₃	H		2.7 ± 1.2%
5e	NH	COOCH ₃	CF ₃		12.6 ± 6.4%
5f	NH	NO ₂	NO ₂		61.7 ± 9.1%
6a	O	NO ₂	CF ₃		18.8 ± 4.0%
6b	NHCO	NO ₂	CF ₃		1.7 ± 6%

Table 2. Cont.

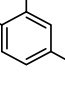

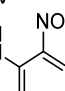

Strategy II					
Compound ID	R ¹	R ²	R ³	R ⁴	% of Kv10.1 Inhibition at 10 μM (HEK-293 Cells)
6c	NH	COOCH ₃	CF ₃		4.2 ± 5.5%
6d	NH	NO ₂	NO ₂		61.9 ± 9.0%
10a	NH	COOH	H		5.8 ± 5.3%
10b	NH	COOH	CF ₃		-2.1 ± 5.7%

Table 3. Structures and potencies of compounds from Strategy III.

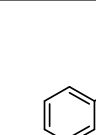
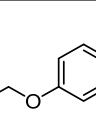
Compound ID	Structure	% of Kv10.1 Inhibition at 10 μM (HEK-293 Cells)
14		3.3 ± 1.7%
15		66.6 ± 4.3%

Table 4. Structures and potencies of compounds from Strategy IV.




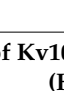


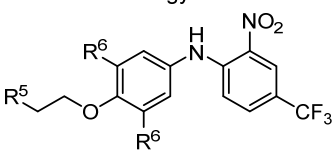
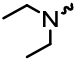
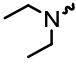
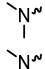
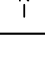
Strategy IV		
Compound ID	R ⁵	% of Kv10.1 Inhibition at 10 μM (HEK-293 Cells)
13		62.4 ± 3.9%
17a		86.2 ± 6.8%
18a		81.4 ± 5.6%
19		68.4 ± 14.8%
20		65 ± 6.0%
21		71.0 ± 4.12%

Table 5. Structures and potencies of compounds from Strategy V.

Strategy V			
			
Compound ID	R ⁵	R ⁶	% of Kv10.1 Inhibition at 1 μM (HEK-293 Cells)
17b		Br	38.2 ± 1.4%
17c		Cl	66.5 ± 5.5%
18b		Br	73.5 ± 0.5%
18c		Cl	28.4 ± 12.1%

It can be concluded that the most potent new diarylamine inhibitors contain a combination of a disubstituted phenyl ring with *para*-trifluoromethyl and *ortho*-nitro groups and a phenyl ring with two *meta*-halogen groups or an unsubstituted phenyl ring. By modifications of the aliphatic chain between the basic centre and the aromatic ring of ZVS-08 (**1**), we succeeded in increasing the potency and the most potent K_V10.1 inhibitors contained a combination of a shorter ethoxy linker and various aliphatic tertiary amines, of which diethylamine or methylamine were optimal.

Diethylamine-containing compound **17a** and dimethylamine-containing compound **18a** from strategy IV and novel 3,5-dibromo-(dimethylamino)ethoxy) analogue **18b** from strategy V were further evaluated for K_V10.1 and hERG inhibition (dose–response curves, Figure 3). Compound **17a** inhibited K_V10.1 with an IC₅₀ value of 568 nM and was more potent than the previously most active compound **2** (IC₅₀ = 740 nM). Compound **17a** was also similarly potent against hERG (IC₅₀ = 232 nM) than **2** (IC₅₀ = 207 nM), allowing us to slightly increase selectivity index against hERG with the new analogue. Compound **18b** was the most potent new K_V10.1 inhibitor (IC₅₀ = 216 nM), but also inhibited hERG very strongly with an IC₅₀ value of 4.9 nM. Increasing the lipophilicity of the molecule by adding two *meta*-halogen groups to the unsubstituted phenyl ring, as in the case of **18b**, increased the potency for both channels but impaired the affinity for hERG considerably more. It appears that the diarylamine core with a disubstituted phenyl ring containing *ortho*-nitro and *para*-trifluoromethyl groups and an unsubstituted phenyl ring is essential for K_V10.1 inhibition, but that with modifications of the alkoxy linker lengths and the basic dimethylamino centre, selectivity toward hERG can be increased.

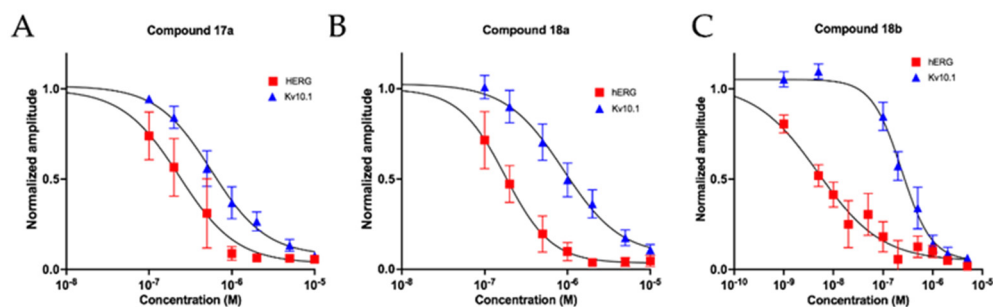


Figure 3. (A) Dose–response curves of compound **17a** for K_V10.1 (blue) and hERG (red) inhibition. The IC₅₀ values from the fit were 568 nM (95% CI 427 to 783 nM N = 4–7) for K_V10.1 and 232 nM (CI: 186 to 296 nM N = 5–6) for hERG. (B) Dose–response curves of compound **18a** for K_V10.1 (blue) and

hERG (red) inhibition. The IC_{50} values from the fit were 892 nM (95% CI 640 nM to 1.40 μ M, N = 5–6) for $K_V10.1$ and 177 nM (CI: 163 to 191 nM, N = 2–3) for hERG. (C) Dose–response curves of compound **18b** for $K_V10.1$ (blue) and hERG (red) inhibition. The IC_{50} values from the fit were 237 nM (95% CI 177 to 331 nM, N = 2–6) for $K_V10.1$ and 4.9 nM (CI: 2.34 to 9.44 nM, N = 2–6) for hERG.

The new analogues were also tested for their $K_V10.1$ and hERG inhibition in another independent assay ex vivo in *Xenopus laevis* oocytes expressing $K_V10.1$ or hERG (Tables S1–S5, Supplementary Materials). Some of the most active compounds (**17a**, **18a**, **18c**, **20**, and **21**) on HEK-293 cells also achieved the highest percentage of $K_V10.1$ in *Xenopus laevis* oocytes. In addition, we determined their IC_{50} values for $K_V10.1$ and hERG and the most potent compound was **17a**, which inhibited $K_V10.1$ currents with an IC_{50} value of 3.6 μ M and hERG currents with an IC_{50} value of 2.0 μ M (Table S4).

3.4. Antiproliferative Activities of Novel $K_V10.1$ Inhibitors **17a** and **18b**

$K_V10.1$ inhibitors are promising candidates that have antiproliferative activity against cancer cell lines expressing this channel. Our new, highly potent $K_V10.1$ inhibitors **17a** and **18b** were tested for their antiproliferative activity against the MCF-7 breast cancer cell line, which has high $K_V10.1$ and low hERG expression. Different concentrations of the compounds were added to the culture medium and the MTS assay was used to determine the number of viable cells after 72 h of incubation. The results obtained are shown in Table 6. Both compounds moderately inhibited the growth of MCF-7 cancer cells. Compound **18b**, which was the most potent $K_V10.1$ inhibitor, inhibited the proliferation of MCF-7 cancer cells with an IC_{50} value of 11.9 μ M. Compound **17a**, whose IC_{50} value for $K_V10.1$ was approximately twice that of **18b**, inhibited proliferation of MCF-7 cancer cells with an IC_{50} value of 18.5 μ M.

Table 6. IC_{50} values for $K_V10.1$, hERG, and the antiproliferative activities in the MCF-7 breast cancer cell line of the synthesized compounds **17a** and **18b**.

Compound ID	IC_{50} [nM] on $K_V10.1$	IC_{50} [nM] on hERG1	IC_{50} [μ M] on MCF-7
17a	568 nM	232 nM	18.5 \pm 1.5
18b	216 nM	4.9 nM	11.9 \pm 1.0

The effect of different concentrations of inhibitors **17a** and **18b** was tested on a cancer cell line with low hERG and high $K_V10.1$ (MCF-7, breast) expression and another cancer cell line with high hERG and very low $K_V10.1$ expression (Panc-1, from pancreas). Cell growth was then monitored over 48–72 h (Figure 4). Both compounds inhibited cancer cell growth to a very similar extent and also with similar potency, reducing proliferation of both cell lines by approximately half at 25 μ M. Higher concentrations up to 100 μ M only slightly increased growth inhibition. The MCF-7 cells were less sensitive to both compounds. The higher sensitivity of Panc-1 cells may be due to the high potency of both compounds in inhibiting hERG (Table 6), which is highly expressed in this cell line and is one of the major ion-channel-encoding genes involved in the initiation and maintenance of neoplastic growth [32,33]. In summary, **17a** and **18b** were able to reduce the growth of cancer cells expressing $K_V10.1$ or hERG, suggesting that both channels contribute to cancer cell proliferation. Therefore, our new inhibitors have a potential anticancer effect.

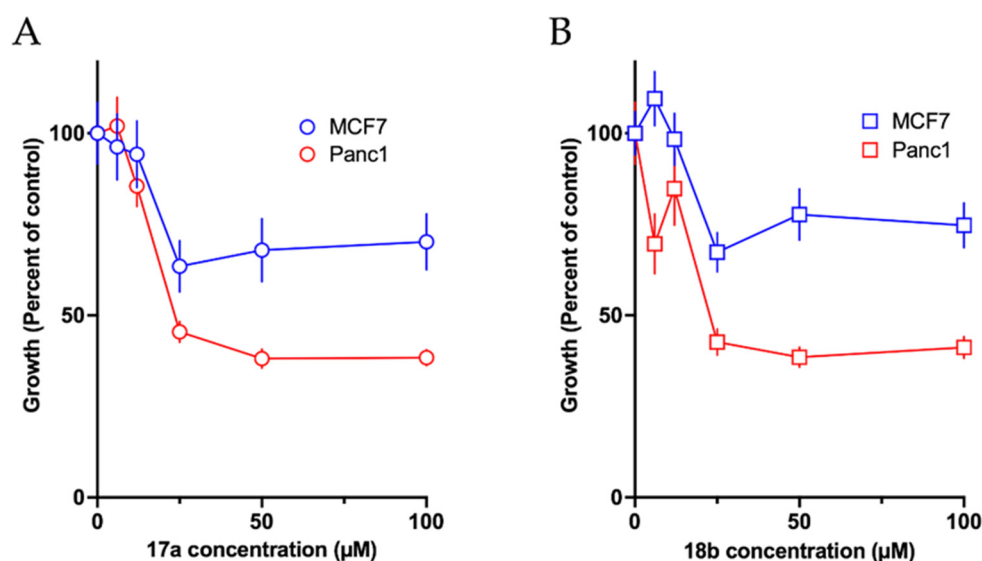


Figure 4. Effects of compounds **17a** and **18b** on the growth of Panc-1 and MCF-7 cells. (A) Compound **17a** inhibited the growth of Panc-1 (red) and MCF-7 cells (blue) by approximately 50% at concentrations higher than 25 µM. The inhibition of growth was stronger on Panc-1 cells. (B) Compound **18b** showed a similar behaviour on both cell lines. Compound **18b** inhibited the growth of Panc-1 cells more potently than MCF-7.

4. Conclusions

Two new potent $K_V10.1$ inhibitors were discovered by structural optimisation of previously published compounds based on the diarylamine scaffold. Important structural elements for the activity of these inhibitors were identified by SAR studies. We learned that the aliphatic chain between the basic centre and the diarylamine scaffold can be modified to increase potency at $K_V10.1$ and improve selectivity toward hERG. The new inhibitor **17a**, with a shorter ethoxy linker and a basic diethylamine centre, showed improved potency ($IC_{50} = 568$ nM) and a better ratio between IC_{50} values for hEAG1 and hERG than previously published diarylamine inhibitors. The most potent analogue of the series, **18b**, inhibited $K_V10.1$ with an IC_{50} value of 216 nM, but also caused significant hERG inhibition. Compounds **17a** and **18b** moderately inhibited the growth of MCF-7 breast cancer cells, which have low hERG and high $K_V10.1$ expression. The new diarylamine $K_V10.1$ inhibitors provided new structural information required for $K_V10.1$ inhibition, but selectivity toward hERG remains a challenge.

Supplementary Materials: The following supporting information can be downloaded at: <https://www.mdpi.com/article/10.3390/pharmaceutics14091963/s1>, Table S1: $K_V1.3$ inhibitory potencies on *Xenopus laevis* oocytes of newly designed and synthesised ZVS-08 (1) analogues (Strategy I), voltage clamped to determine the percentage of inhibition at 10 µM; Table S2: $K_V1.3$ inhibitory potencies on *Xenopus laevis* oocytes of newly designed and synthesised ZVS-08 (1) analogues (Strategy II), voltage clamped to determine the percentage of inhibition at 10 µM on $K_V10.1$ and hERG; Table S3: $K_V1.3$ inhibitory potencies on *Xenopus laevis* oocytes of newly designed and synthesised ZVS-08 (1) analogues (Strategy II), voltage clamped to determine the percentage of inhibition at 10 µM on $K_V10.1$ and hERG; Table S4: $K_V1.3$ inhibitory potencies on *Xenopus laevis* oocytes of newly designed and synthesised ZVS-08 (1) analogues (Strategy IV), voltage clamped to determine the percentage of inhibition at 10 µM on $K_V10.1$ and hERG; Table S5: $K_V1.3$ inhibitory potencies on *Xenopus laevis* oocytes of newly designed and synthesised ZVS-08 (1) analogues (Strategy V), voltage clamped to determine the percentage of inhibition at 10 µM on $K_V10.1$ and hERG.

Author Contributions: Conceptualization, Š.G., L.P.M., L.A.P. and T.T.; methodology, L.P.M., L.A.P. and T.T.; formal analysis, Š.G., X.S., L.A.H., E.L.P.-J., J.D. and L.A.P.; investigation, Š.G., L.A.H., E.L.P.-J., X.S., T.T. and L.A.P.; data curation, Š.G., L.A.H., X.S., E.L.P.-J., Ž.T., S.P., T.T. and L.A.P.; writing—original draft preparation, Š.G., T.T., L.A.P. and L.P.M.; writing—review and editing, Š.G., J.T., T.T., L.A.P. and L.P.M.; supervision, S.P., J.T., T.T., L.A.P. and L.P.M.; project administration, J.T., T.T., L.A.P. and L.P.M.; funding acquisition, J.T., L.A.P. and L.P.M. All authors have read and agreed to the published version of the manuscript.

Funding: This research was funded by the Slovenian Research Agency (ARRS) grant numbers J1-9192, N1-0098, P1-0208 and CELSA project. The work also received funding from the Max-Planck Society and from the European Union through Horizon 2020 research and innovation programme under the Marie Skłodowska-Curie grant agreement No. 813834-PHIONIC-H2020-MSCA-ITN-2018. This study was supported by grants GOE7120N, GOC2319N, and GOA4919N from the F.W.O. Vlaanderen, awarded to J.T. and S.P. was supported by KU Leuven funding (PDM/19/164) and F.W.O. Vlaanderen grant 12W7822N.

Institutional Review Board Statement: The use of *Xenopus laevis* was approved by the Animal Ethics Committee of the KU Leuven (Project nr. P186/2019).

Informed Consent Statement: Not applicable.

Data Availability Statement: The data presented in this study are available on request from the corresponding author.

Acknowledgments: We thank OpenEye Scientific Software, Santa Fe, NM, USA, for free academic licenses for the use of their software. L.A.P. thanks the expert technical assistance of V. Díaz.

Conflicts of Interest: The authors declare that they have no conflict of interest.

Appendix A

General procedure for synthesis of phenoxyphenol intermediates **3a–b** (**3a** is given as example)

Synthesis of methyl 2-(4-hydroxyphenoxy)benzoate (**3a**): To a stirring solution of methyl 2-bromobenzoate (2.14 g, 9.95 mmol) in pyridine (50 mL), hydroquinone (1.10 g, 9.95 mmol), K_2CO_3 (2.75 g, 19.90 mmol), and CuO (80 mg, 1.00 mmol) were added. The batch was stirred at 110 °C for 72 h and then cooled to room temperature and filtered through Celite. The solvent was removed under reduced pressure and the crude product was purified by flash column chromatography using ethyl acetate/hexane = 1:1 as a mobile phase.

Methyl 2-(4-hydroxyphenoxy)benzoate (**3a**): Yield: 10%; white solid (250 mg); 1H NMR (400 MHz, $CDCl_3$) δ 7.87 (dd, $J_1 = 7.8$ Hz, $J_2 = 1.8$ Hz, 1 H), 7.44–7.37 (m, 1 H), 7.11 (td, $J_1 = 7.7$ Hz, $J_2 = 1.0$ Hz, 1 H), 6.91–6.85 (m, 3 H), 6.83–6.78 (m, 2 H), 4.90 (brs, 1 H), and 3.86 (s, 3 H).

4-(2-Nitro-4-(trifluoromethyl)phenoxy)phenol (**3b**): Synthesised from 1-chloro-2-nitro-4-(trifluoromethyl)benzene (4.00 g, 17.73 mmol), hydroquinone (1.95 g, 17.73 mmol), K_2CO_3 (7.35 g, 53.20 mmol), and CuO (141 mg, 1.77 mmol) in pyridine (50 mL). Purified by flash column chromatography using ethyl acetate/hexane = 1:1 as mobile phase. Yield: 67%; yellow solid (3.565 g); 1H NMR (400 MHz, $CDCl_3$) δ 8.21 (d, $J = 2.0$ Hz, 1 H), 7.73–7.62 (m, 1 H), 7.03–6.96 (m, 3 H), 6.95–6.87 (m, 2 H), and 6.22 (brs, 1 H).

General procedure for binding of epichlorohydrin to phenol intermediates to obtain **4a–4g** (**4a** is given as example)

To the argon-flushed solution of **3a** (250 mg, 1.02 mmol) in MeCN (40 mL) on ice bath K_2CO_3 (423 mg, 3.06 mmol) and (\pm)-epichlorohydrin (0.94 g, 10.20 mmol, 0.80 mL) were added. Reaction mixture was stirred at 80 °C for 16 h. K_2CO_3 was filtered off and the solvent was removed under reduced pressure. Crude product was purified with flash column chromatography using ethyl acetate/hexane = 1:1 as eluent to obtain **4a** (428 mg).

Methyl 2-(4-(oxiran-2-ylmethoxy)phenoxy)benzoate (**4a**): Yield: 91%; white solid (280 mg); 1H NMR (400 MHz, $CDCl_3$) δ 7.88 (dd, $J_1 = 7.8$ Hz, $J_2 = 1.8$ Hz, 1 H), 7.41 (ddd, $J_1 = 8.3$ Hz, $J_2 = 7.4$ Hz, $J_3 = 1.8$ Hz, 1 H), 7.12 (td, $J_1 = 7.7$ Hz, $J_2 = 1.1$ Hz, 1 H), 6.98–6.85 (m,

5 H), 4.21 (dd, $J_1 = 11.0$ Hz, $J_2 = 3.1$ Hz, 1 H), 3.93 (dd, $J_1 = 11.0$ Hz, $J_2 = 5.7$ Hz, 1 H), 3.85 (s, 3 H), 3.35 (ddt, $J_1 = 5.7$ Hz, $J_2 = 4.1$ Hz, $J_3 = 3.0$ Hz, 1 H), 2.91 (dd, $J_1 = 4.9$ Hz, $J_2 = 4.2$ Hz, 1 H), and 2.76 (dd, $J_1 = 4.9$ Hz, $J_2 = 2.7$ Hz, 1 H).

2-((4-(2-Nitro-4-(trifluoromethyl)phenoxy)phenoxy)methyl)oxirane (**4b**): Synthesised from 4-(2-nitro-4-(trifluoromethyl)phenoxy)phenol (**3b**) (3.55 g, 11.87 mmol, 1.0 equiv) with 10 equivalents of (\pm)-epichlorohydrin and 3 equivalents of K_2CO_3 . Purified with flash column chromatography using ethyl acetate/hexane = 1:2 as mobile phase. Yield: 61.1%; yellow oil (1.45 g); 1H NMR (400 MHz, DMSO) δ 8.44 (d, $J = 2.0$ Hz, 1 H), 8.02–7.92 (m, 1 H), 7.24–7.15 (m, 2 H), 7.13–7.03 (m, 3 H), 4.36 (dd, $J_1 = 11.4$ Hz, $J_2 = 2.6$ Hz, 1 H), 3.86 (dd, $J_1 = 11.4$ Hz, $J_2 = 6.6$ Hz, 1 H), 3.37–3.33 (m, 1 H), 2.86 (dd, $J_1 = 5.0$ Hz, $J_2 = 4.3$ Hz, 1 H), and 2.72 (dd, $J_1 = 5.1$ Hz, $J_2 = 2.7$ Hz, 1 H).

2-Nitro-*N*-(4-(oxiran-2-ylmethoxy)phenyl)-4-(trifluoromethyl)benzamide (**4c**): Synthesised from *N*-(4-hydroxyphenyl)-2-nitro-4-(trifluoromethyl)benzamide (**7**) (1.60 g, 4.90 mmol) and 10 equivalents of (\pm)-epichlorohydrin and purified with flash column chromatography using ethyl acetate/hexane = 1:1 as eluent and with dry sample loading. Yield: 33%; red crystals (618 mg); 1H NMR (400 MHz, DMSO) δ 10.66 (s, 1 H), 8.50 (s, 1 H), 8.28 (dd, $J_1 = 8.0$ Hz, $J_2 = 1.1$ Hz, 1 H), 8.03 (d, $J = 7.9$ Hz, 1 H), 7.65–7.51 (m, 2 H), 7.04–6.92 (m, 2 H), 4.32 (dd, $J_1 = 11.4$ Hz, $J_2 = 2.7$ Hz, 1 H), 3.82 (dd, $J_1 = 11.4$ Hz, $J_2 = 6.5$ Hz, 1 H), 3.36–3.33 (m, 1 H), 2.87–2.81 (m, 1 H), and 2.71 (dd, $J_1 = 5.1$ Hz, $J_2 = 2.7$ Hz, 1 H).

Methyl 2-((4-(oxiran-2-ylmethoxy)phenyl)amino)benzoate (**4d**): resynthesized according to described procedures [26].

Methyl 2-((4-(oxiran-2-ylmethoxy)phenyl)amino)-5-(trifluoromethyl)benzoate (**4e**): Synthesised from methyl 2-((4-hydroxyphenyl)amino)-5-(trifluoromethyl)benzoate (**9b**) (330 mg, 1.06 mmol, 1.0 equiv.) with 10 equivalents of (\pm)-epichlorohydrin and purified with flash column chromatography using ethyl acetate/hexane = 1:4 as eluent. Yield: 72%; white solid (281 mg); 1H NMR (400 MHz, DMSO) δ 9.49 (s, 1 H), 8.10 (d, $J = 1.7$ Hz, 1 H), 7.63 (dd, $J_1 = 9.0$ Hz, $J_2 = 2.3$ Hz, 1 H), 7.29–7.19 (m, 2 H), 7.08–7.00 (m, 2 H), 6.97 (d, $J = 9.0$ Hz, 1 H), 4.35 (dd, $J_1 = 11.4$ Hz, $J_2 = 2.6$ Hz, 1 H), 3.89 (s, 3 H), 3.88–3.80 (m, 1 H), 3.40–3.33 (m, 1 H), 2.86 (dd, $J_1 = 5.0$ Hz, $J_2 = 4.3$ Hz, 1 H), and 2.72 (dd, $J_1 = 5.1$ Hz, $J_2 = 2.7$ Hz, 1 H).

2-Nitro-*N*-(4-(oxiran-2-ylmethoxy)phenyl)-4-(trifluoromethyl)aniline (**4f**): resynthesized according to described procedures [26].

2,4-Dinitro-*N*-(4-(oxiran-2-ylmethoxy)phenyl)aniline (**4g**): Synthesised from 4-((2,4-dinitrophenyl)amino)phenol (**12b**) (1.93 g, 7.0 mmol, 1.0 equiv.), 10 equivalents of (\pm)-epichlorohydrin and K_2CO_3 (2.91 g, 21.1 mmol, 3.0 equiv.). Purified with flash column chromatography ethyl acetate/hexane = 1:1 as eluent. Yield: 78%; red solid (1.8 g); 1H NMR (400 MHz, DMSO) δ 10.10 (s, 1 H), 8.89 (d, $J = 2.7$ Hz, 1 H), 8.20 (dd, $J_1 = 9.6$ Hz, $J_2 = 2.8$ Hz, 1 H), 7.38–7.23 (m, 2 H), 7.16–7.04 (m, 2 H), 6.96 (d, $J = 9.6$ Hz, 1 H), 4.39 (dd, $J_1 = 11.4$ Hz, $J_2 = 2.6$ Hz, 1 H), 3.88 (dd, $J_1 = 11.4$ Hz, $J_2 = 6.6$ Hz, 1 H), 3.43–3.32 (m, 1 H), 2.87 (dd, $J_1 = 5.0$ Hz, $J_2 = 4.3$ Hz, 1 H), and 2.73 (dd, $J_1 = 5.1$, $J_2 = 2.7$ Hz, 1 H).

General procedure for opening of the epoxide with morpholine to obtain **5a–5f** (**5a** is given as example)

To a stirring solution of methyl 2-(4-(oxiran-2-ylmethoxy)phenoxy)benzoate (**4a**) (100 mg, 0.333 mmol) in acetonitrile (20 mL), morpholine (87 mg, 0.999 mmol, 0.086 mL, 3.0 equiv.) was added and stirred for 72 h at room temperature. After 72 h, solvent was removed under reduced pressure and product was purified with flash column chromatography using dichloromethane/methanol/ammonium = 20:1:0.1.

Methyl 2-(4-(2-hydroxy-3-morpholinopropoxy)phenoxy)benzoate (**5a**): Yield: 40%; white solid (50 mg); 1H NMR (400 MHz, MeOD) δ 7.82 (dd, $J_1 = 7.8$ Hz, $J_2 = 1.7$ Hz, 1 H), 7.45 (ddd, $J_1 = 8.4$ Hz, $J_2 = 7.4$ Hz, $J_3 = 1.8$ Hz, 1 H), 7.13 (td, $J_1 = 7.7$ Hz, $J_2 = 1.0$ Hz, 1 H), 6.99–6.88 (m, 4 H), 6.85 (dd, $J_1 = 8.3$ Hz, $J_2 = 0.8$ Hz, 1 H), 4.87 (brs, 1 H), 4.12 (ddd, $J_1 = 9.2$ Hz, $J_2 = 7.4$ Hz, $J_3 = 5.3$ Hz, 1 H), 3.99 (dd, $J_1 = 9.7$ Hz, $J_2 = 4.1$ Hz, 1 H), 3.91 (dd, $J_1 = 9.8$ Hz, $J_2 = 5.9$ Hz, 1 H), 3.80 (s, 3 H), 3.74–3.60 (m, 4 H), 2.62–2.47 (m, 6 H); ^{13}C NMR (101 MHz, MeOD) δ 168.01, 158.65, 156.71, 151.89, 134.71, 132.55, 123.76, 123.47, 121.21,

120.07, 116.78, 72.42, 68.11, 67.78, 62.57, 55.35, and 52.62; HRMS (ESI⁺) for C₂₁H₂₆NO₆ ([M+H]⁺) calculated 388.1755 found 388.1745; HPLC retention time: 2.793 min (96.90% at 254 nm).

1-Morpholino-3-(4-(2-nitro-4-(trifluoromethyl)phenoxy)phenoxy)propan-2-ol (**5b**): Synthesised from 2-((4-(2-nitro-4-(trifluoromethyl)phenoxy)phenoxy)methyl)oxirane (**4b**) (500 mg, 1.41 mmol) in acetonitrile (30 mL) and three equivalents of morpholine (368 mg, 4.22 mmol, 0.364 mL). Purified with flash column chromatography using dichloromethane/methanol: 20/1 as eluent. Yield: 21%; yellow oil (130 mg); ¹H NMR (400 MHz, CDCl₃) δ 8.21 (d, *J* = 1.9 Hz, 1 H), 7.71–7.64 (m, 1 H), 7.09–7.03 (m, 2 H), 6.99 (dt, *J*₁ = 5.7 Hz, *J*₂ = 3.3 Hz, 3 H), 4.18 (dq, *J*₁ = 9.2 Hz, *J*₂ = 4.7 Hz, 1 H), 4.05–3.95 (m, 2 H), 3.85–3.70 (m, 5 H), 2.81–2.71 (m, 2 H), 2.70–2.60 (m, 2 H), 2.60–2.52 (m, 2 H); ¹³C NMR (101 MHz, CDCl₃) δ 156.71, 154.78, 147.72, 139.90, 130.86 (q, *J* = 3.4 Hz), 124.52 (q, *J* = 34.5 Hz), 123.64 (q, *J* = 3.9 Hz), 123.01 (q, *J* = 271.0 Hz), 121.80, 118.60, 116.27, 70.77, 66.86, 65.34, 61.18, and 53.87. HRMS (ESI⁺) for C₂₀H₂₂F₃N₂O₆ ([M+H]⁺) calculated 443.1425 found 443.1415; HPLC retention time: 3.600 min (98.51% at 254 nm).

N-(4-(2-Hydroxy-3-morpholinopropoxy)phenyl)-2-nitro-4-(trifluoromethyl)benzamide (**5c**): Synthesised from 2-nitro-*N*-(4-(oxiran-2-ylmethoxy)phenyl)-4-(trifluoromethyl)benzamide (**4c**) (300 mg, 0.78 mmol, 1.0 equiv.) and three equivalents of morpholine in dichloromethane (40 mL). Reaction was stopped after 72 h. Mobile phase for flash column chromatography was dichloromethane/methanol: 20/1. Yield: 41%; yellow solid (150 mg); ¹H NMR (400 MHz, DMSO) δ 10.63 (s, 1 H), 8.50 (d, *J* = 1.0 Hz, 1 H), 8.28 (dd, *J*₁ = 8.0 Hz, *J*₂ = 1.1 Hz, 1 H), 8.02 (d, *J* = 7.9 Hz, 1 H), 7.59–7.49 (m, 2 H), 7.00–6.91 (m, 2 H), 4.87 (d, *J* = 4.5 Hz, 1 H), 4.00–3.92 (m, 2 H), 3.86 (dd, *J*₁ = 11.0 Hz, *J*₂ = 7.3 Hz, 1 H), 3.57 (t, *J* = 4.6 Hz, 4 H), 2.48–2.30 (m, 6 H); ¹³C NMR (101 MHz, MeOD) δ 165.61, 157.71, 147.99, 137.53, 133.66 (q, *J* = 34.2 Hz), 132.56, 131.82 (q, *J* = 3.4 Hz), 131.62, 124.20 (q, *J* = 271.0 Hz), 123.34, 122.88 (q, *J* = 3.8 Hz), 115.91, 72.19, 68.17, 67.84, 62.60, and 55.40. HRMS (ESI⁺) for C₂₁H₂₃F₃N₃O₆ ([M+H]⁺) calculated 470.1534 found 470.1523; HPLC retention time: 2.930 min (99.76% at 254 nm).

Methyl 2-((4-(2-hydroxy-3-morpholinopropoxy)phenyl)amino)benzoate (**5d**): Synthesised from methyl 2-((4-(oxiran-2-ylmethoxy)phenyl)amino)benzoate (**4d**) (590 mg, 1.97 mmol, 1.0 equiv.) and three equivalents of morpholine (515 mg, 5.91 mmol, 0.512 mL) for 72 h at room temperature. Purified with flash column chromatography using ethyl acetate/hexane = 2:1 and one more column with dichloromethane/methanol/ammonium = 20:1:0.1 as eluent and dry sample loading. Yield: 32%; yellow oil (240 mg); ¹H NMR (400 MHz, DMSO) δ 9.15 (s, 1 H), 7.86 (dd, *J*₁ = 8.0 Hz, *J*₂ = 1.6 Hz, 1 H), 7.34 (ddd, *J*₁ = 8.6 Hz, *J*₂ = 7.2 Hz, *J*₃ = 1.6 Hz, 1 H), 7.21–7.13 (m, 2 H), 7.00–6.95 (m, 2 H), 6.93 (dd, *J*₁ = 8.6 Hz, *J*₂ = 0.7 Hz, 1 H), 6.71 (ddd, *J*₁ = 8.1 Hz, *J*₂ = 7.1 Hz, *J*₃ = 1.1 Hz, 1 H), 4.87 (d, *J* = 4.7 Hz, 1 H), 4.01–3.92 (m, 2 H), 3.87 (dd, *J*₁ = 10.0 Hz, *J*₂ = 6.4 Hz, 1 H), 3.85 (s, 3 H), 3.56 (t, *J* = 4.6 Hz, 4 H), 2.48–2.31 (m, 6 H). ¹³C NMR (101 MHz, MeOD) δ 170.24, 157.48, 150.64, 135.28, 134.88, 132.56, 126.63, 117.38, 116.53, 114.31, 112.04, 72.22, 68.14, 67.81, 62.61, 55.38, and 52.16; HRMS (ESI⁺) for C₂₁H₂₇N₂O₅ ([M+H]⁺) calculated 387.1915 found 387.1905; HPLC retention time: 3.940 min (98.44% at 254 nm).

Methyl 2-((4-(2-hydroxy-3-morpholinopropoxy)phenyl)amino)benzoate (**5e**): Synthesised from methyl 2-((4-(oxiran-2-ylmethoxy)phenyl)amino)-5-(trifluoromethyl)benzoate (**4e**) (590 mg, 1.97 mmol) with three equivalents of morpholine (100 mg, 1.14 mmol, 0.099 mL) at room temperature for 72 h. Purified with flash column chromatography using ethyl acetate/hexane = 1:4. Yield: 11%; yellow oil (100 mg); ¹H NMR (400 MHz, CDCl₃) δ 9.57 (s, 1 H), 8.21 (d, *J* = 1.4 Hz, 1 H), 7.43 (dd, *J*₁ = 9.0 Hz, *J*₂ = 2.2 Hz, 1 H), 7.21–7.12 (m, 2 H), 7.02–6.89 (m, 3 H), 4.13 (tt, *J*₁ = 9.5 Hz, *J*₂ = 4.9 Hz, 1 H), 4.05–3.97 (m, 2 H), 3.93 (s, 3 H), 3.81–3.66 (m, 4 H), 2.76–2.64 (m, 2 H), 2.64–2.53 (m, 2 H), 2.54–2.43 (m, 2 H); ¹³C NMR (101 MHz, CDCl₃) δ 168.38, 156.75, 151.92, 132.51, 130.71 (q, *J* = 3.3 Hz), 129.46 (q, *J* = 3.9 Hz), 124.50 (q, *J* = 270.6 Hz), 126.74, 117.98 (q, *J* = 33.2 Hz), 115.69, 113.42, 109.99, 70.64, 67.15, 65.52, 61.14, 53.90, and 52.16; HRMS (ESI⁺) for C₂₂H₂₆F₃N₂O₅ ([M+H]⁺) calculated 455.1788 found 455.1777; HPLC retention time: 3.953 min (96.49% at 254 nm).

1-(4-((2,4-Dinitrophenyl)amino)phenoxy)-3-morpholinopropan-2-ol (**5f**): Synthesised from 2,4-dinitro-*N*-(4-(oxiran-2-ylmethoxy)phenyl)aniline (**4g**) (442 mg, 1.34 mmol, 1.0 equiv.) with morpholine (465 mg, 5.34 mmol, 0.470 mL, 4.0 equiv.) in acetonitrile (50 mL) at room temperature for 72 h. Purified with flash column chromatography using dichloromethane/methanol/ $\text{NH}_3 = 20:1:0.01$ as eluent and Biotage Isolera One System reversed-phase chromatography (Biotage SNAP Cartridge KP-C18-HS 12 g column), MF: gradient 0,1% trifluoroacetic acid in H_2O /acetonitrile). Yield: 18%; red amorph solid (100 mg); ^1H NMR (400 MHz, CDCl_3) δ 9.87 (s, 1 H), 9.17 (d, $J = 2.6$ Hz, 1 H), 8.21–8.07 (m, 1 H), 7.25–7.19 (m, 2 H), 7.09–6.94 (m, 3 H), 4.16 (td, $J_1 = 9.4$ Hz, $J_2 = 4.5$ Hz, 1 H), 4.09–3.98 (m, 2 H), 3.85–3.68 (m, 4 H), 2.79–2.44 (m, 6 H); ^{13}C NMR (101 MHz, CDCl_3) δ 158.35, 148.03, 137.24, 130.88, 130.01, 129.64, 127.59, 124.25, 116.19, 116.09, 70.69, 67.10, 65.39, 61.03, and 53.86; HRMS (ESI⁺) for $\text{C}_{19}\text{H}_{23}\text{N}_4\text{O}_7$ ($[\text{M}+\text{H}]^+$) calculated 419.1561 found 419.1550; HPLC retention time: 3.430 min (99.08% at 254 nm).

General procedure for opening of the epoxide with dimethylamine to obtain **6a–6d** (**6a** is given as example)

To a stirring solution of methyl 2-(4-(oxiran-2-ylmethoxy)phenoxy)benzoate (**4b**) (500 mg, 1.4 mmol, 1.0 equiv) in acetonitrile (30 mL), $\text{Me}_2\text{NH} \times \text{HCl}$ (460 mg, 5.63 mmol, 4.0 equiv) and K_2CO_3 (580 mg, 4.2 mmol, 3.0 equiv) were added and the batch was stirred at 70 °C for 24 h. The solvent was removed under reduced pressure and the crude product was purified with Biotage Isolera One System reversed-phase chromatography (Biotage SNAP Cartridge KP-C18-HS 12 g column), MF: gradient 0,1% trifluoroacetic acid in H_2O /acetonitrile). Fractions containing 1-(dimethylamino)-3-(4-(2-nitro-4-(trifluoromethyl)phenoxy)phenoxy)propan-2-ol (**6a**) were combined, acetonitrile was removed under reduced pressure and pH of remaining water phase was set to 8, and product was extracted into ethyl acetate (2 × 25 mL). Organic phase was washed with brine (2 × 25 mL) dried over Na_2SO_4 filtered and the solvent removed under reduced pressure to obtain **6a** (100 mg).

1-(Dimethylamino)-3-(4-(2-nitro-4-(trifluoromethyl)phenoxy)phenoxy)propan-2-ol (**6a**): Yield: 18%; yellow oil (100 mg); ^1H NMR (400 MHz, CDCl_3) δ 8.19 (d, $J = 1.8$ Hz, 1 H), 7.68 (dd, $J_1 = 8.9$ Hz, $J_2 = 2.0$ Hz, 1 H), 7.09–6.93 (m, 5 H), 4.36 (brs, 1 H), 4.22–4.13 (m, 1 H), 4.01 (d, $J = 4.9$ Hz, 2 H), 2.77–2.67 (m, 1 H), 2.55 (dd, $J_1 = 12.4$ Hz, $J_2 = 2.7$ Hz, 1 H), 2.45 (s, 6 H); ^{13}C NMR (101 MHz, CDCl_3) δ 156.43, 154.67, 147.80, 139.85, 130.95 (q, $J = 3.7$ Hz), 124.55 (q, $J = 34.5$ Hz), 123.60 (q, $J = 3.8$ Hz), 123.02 (q, $J = 271.0$ Hz), 121.75, 118.73, 116.30, 70.54, 65.41, 61.62, and 45.07; HRMS (ESI⁺) for $\text{C}_{18}\text{H}_{20}\text{F}_3\text{N}_2\text{O}_5$ ($[\text{M}+\text{H}]^+$) calculated 401.1319 found 401.1310; HPLC retention time: 3.593 min (95.01% at 254 nm).

N-(4-(3-(Dimethylamino)-2-hydroxypropoxy)phenyl)-2-nitro-4-(trifluoromethyl)benzamide (**6b**): Synthesised from 2-nitro-*N*-(4-(oxiran-2-ylmethoxy)phenyl)-4-(trifluoromethyl)benzamide (**4c**) (300 mg, 0.78 mmol) and six equivalents of $\text{Me}_2\text{NH} \times \text{HCl}$ in acetonitrile (40 mL). Purified with Biotage Isolera One System reversed-phase chromatography (Biotage SNAP Cartridge KP-C18-HS 12 g column), MF: gradient 0,1% trifluoroacetic acid in H_2O /acetonitrile). Yield: 27%; yellow solid (90 mg); ^1H NMR (400 MHz, DMSO) δ 10.77 (s, 1 H), 9.82 (s, 1 H), 8.50 (d, $J = 0.9$ Hz, 1 H), 8.28 (dd, $J_1 = 8.0$ Hz, $J_2 = 1.1$ Hz, 1 H), 8.03 (d, $J = 7.9$ Hz, 1 H), 7.64–7.53 (m, 2 H), 7.04–6.91 (m, 2 H), 6.00 (d, $J = 3.9$ Hz, 1 H), 4.29 (d, $J = 2.5$ Hz, 1 H), 4.02–3.88 (m, 2 H), 3.40–3.13 (m, 2 H), 2.84 (d, $J = 11.5$ Hz, 6 H); ^{13}C NMR (101 MHz, MeOD) δ 165.70, 157.18, 148.00, 137.49, 133.73 (q, $J = 34.2$ Hz), 133.05, 131.86 (q, $J = 3.5$ Hz), 130.79, 123.76 (q, $J = 271.0$ Hz), 123.40, 122.90 (q, $J = 3.3$ Hz), 115.94, 71.30, 65.37, and 61.01. HRMS (ESI⁺) for $\text{C}_{19}\text{H}_{21}\text{F}_3\text{N}_3\text{O}_5$ ($[\text{M}+\text{H}]^+$) calculated 428.1428 found 428.1420; HPLC retention time: 2.893 min (97.37% at 254 nm).

Methyl 2-((4-(3-(dimethylamino)-2-hydroxypropoxy)phenyl)amino)-5-(trifluoromethyl)benzoate (**6c**): Synthesised from methyl 2-((4-(oxiran-2-ylmethoxy)phenyl)amino)-5-(trifluoromethyl)benzoate (**4e**) (140 mg, 0.381 mmol), K_2CO_3 (157 mg, 1.14 mmol, 3.0 equiv.) and $\text{Me}_2\text{NH} \times \text{HCl}$ (186 mg, 2.28 mmol, 6.0 equiv) in acetonitrile (35 mL) at 70 °C overnight. Yield: 64%; yellow oil (100 mg); ^1H NMR (400 MHz, CDCl_3) δ 9.56 (s, 1 H), 8.21 (d, $J = 1.4$ Hz, 1 H), 7.42 (dd, $J_1 = 9.0$ Hz, $J_2 = 2.3$ Hz, 1 H), 7.21–7.10 (m, 2 H), 7.02–6.90 (m, 3 H), 4.12–4.04 (m, 1 H),

4.03–3.96 (m, 2 H), 3.93 (s, 3 H), 2.63–2.50 (m, 1 H), 2.40 (dd, $J_1 = 12.2$ Hz, $J_2 = 3.8$ Hz, 1 H), 2.34 (s, 6 H). ^{13}C NMR (101 MHz, CDCl_3) δ 168.32, 156.81, 151.90, 132.36, 130.66 (q, $J = 3.2$ Hz), 129.40 (q, $J = 3.9$ Hz), 126.68, 124.48 (q, $J = 270.6$ Hz), 117.87 (q, $J = 33.2$ Hz), 115.66, 113.40, 109.92, 70.84, 66.31, 61.92, 52.11, and 45.67; HRMS (ESI⁺) $\text{C}_{20}\text{H}_{24}\text{F}_3\text{N}_2\text{O}_4$ ($[\text{M}+\text{H}]^+$) calculated 413.1683 found 413.1672; HPLC retention time: 3.950 min (98.29% at 254 nm).

1-(Dimethylamino)-3-(4-((2,4-dinitrophenyl)amino)phenoxy)propan-2-ol (**6d**): Synthesised from 2,4-dinitro-*N*-(4-(oxiran-2-ylmethoxy)phenyl)aniline (**4g**) (170 mg, 0.706 mmol, 1.0 equiv.), $\text{Me}_2\text{NH} \times \text{HCl}$ (344 mg, 4.220 mmol, 6.0 equiv.) and K_2CO_3 (291 mg, 2.110 mmol, 3.0 equiv.) in acetonitrile (30 mL) at 70 °C for 24 h. Purified with flash column chromatography using dichloromethane/methanol/ $\text{NH}_3 = 20:1:0.01$ as eluent and Biotage Isolera One System reversed-phase chromatography (Biotage SNAP Cartridge KP-C18-HS 12 g column), MF: gradient 0.1% trifluoroacetic acid in H_2O /acetonitrile. Yield: 30%; red solid (80 mg); ^1H NMR (400 MHz, DMSO) δ 10.09 (s, 1 H), 8.89 (d, $J = 2.7$ Hz, 1 H), 8.20 (dd, $J_1 = 9.6$ Hz, $J_2 = 2.8$ Hz, 1 H), 7.33–7.22 (m, 2 H), 7.12–7.04 (m, 2 H), 6.97 (d, $J = 9.6$ Hz, 1 H), 4.88 (d, $J = 3.8$ Hz, 1 H), 4.02 (dd, $J_1 = 9.0$ Hz, $J_2 = 2.9$ Hz, 1 H), 3.97–3.86 (m, 2 H), 2.46–2.27 (m, 2 H), and 2.21 (s, 6 H); ^{13}C NMR (101 MHz, CDCl_3) δ 158.39, 148.03, 137.16, 130.80, 129.97, 129.51, 127.53, 124.19, 116.16, 116.11, 70.86, 66.15, 61.78, and 45.65. HRMS (ESI⁺) for $\text{C}_{17}\text{H}_{21}\text{N}_4\text{O}_6$ ($[\text{M}+\text{H}]^+$) calculated 377.1456 found 377.1447; HPLC retention time: 3.460 min (99.44% at 254 nm).

Synthesis of amide intermediate 7

To a solution of 2-nitro-4-(trifluoromethyl)benzoic acid (3.00 g, 12.76 mmol, 1.0 equiv.) in dichloromethane (100 mL), two drops of DMF and oxalyl chloride (4.86 g, 38.28 mmol, 3.28 mL, 3.0 equiv.) were added while ice cooling and the batch was stirred at 40 °C for 24 h. Solvent was removed under reduced pressure and crude product was resolved in the acetonitrile (20 mL) on the ice bath. To the ice cooled solution, 4-aminophenol (1.67 g, 15.31 mmol, 1.2 equiv.) and triethylamine (3.87 g, 51.04 mmol, 5.33 mL, 3.0 equiv.) were added dropwise and then reaction mixture was heated at reflux overnight. The solvent was removed under reduced pressure. Product was further purified using flash column chromatography with ethyl acetate/hexane = 1:2 as mobile phase and with dry sample loading.

N-(4-Hydroxyphenyl)-2-nitro-4-(trifluoromethyl)benzamide (**7**): Yield: 38%; red solid (1.6 g); ^1H NMR (400 MHz, DMSO) δ 10.52 (s, 1 H), 9.34 (s, 1 H), 8.49 (d, $J = 0.8$ Hz, 1 H), 8.26 (dd, $J_1 = 8.0$ Hz, $J_2 = 1.1$ Hz, 1 H), 8.00 (d, $J = 7.9$ Hz, 1 H), 7.49–7.36 (m, 2 H), and 6.83–6.68 (m, 2 H).

General procedure for synthesis of benzoic acid derivatives **8a–b** (**8a** is given as example)

To an argon-flushed solution of 2-bromobenzoic acid (4.00 g, 19.90 mmol, 1.0 equiv.) in 2-ethoxyethanol (20 mL), CuO (63 mg, 0.80 mmol, 0.04 equiv.), Cu (114 mg, 1.79 mmol, 0.09 equiv.), K_2CO_3 (5.50 g, 39.80 mmol), and 4-aminophenol (2.28 g, 20.89 mmol, 1.05 equiv.) were added and the batch was stirred at 130 °C for 16 h. Solution was cooled to room temperature and then water (100 mL) was added. Mixture was filtered through Celite and then pH was set to 5 to precipitate black solid that was filtered off. Black precipitate was dissolved in the 5% solution of Na_2CO_3 (250 mL) and solution was filtered through Celite. pH in solution was then set to 5 to precipitate black solid that was filtered off and dried overnight.

2-((4-Hydroxyphenyl)amino)benzoic acid (**8a**): Yield: 50%; black solid (2.28 g); ^1H NMR (400 MHz, DMSO) δ 12.90 (s, 1 H), 9.42 (brs, 1 H), 9.34 (brs, 1 H), 7.84 (dd, $J_1 = 8.0$ Hz, $J_2 = 1.6$ Hz, 1 H), 7.30 (ddd, $J_1 = 8.7$ Hz, $J_2 = 7.1$ Hz, $J_3 = 1.7$ Hz, 1 H), 7.08–7.02 (m, 2 H), 6.86 (dd, $J_1 = 8.5$ Hz, $J_2 = 0.7$ Hz, 1 H), 6.83–6.77 (m, 2 H), and 6.69–6.62 (m, 1 H).

2-((4-Hydroxyphenyl)amino)-5-(trifluoromethyl)benzoic acid (**8b**): Synthesised from 2-bromo-5-(trifluoromethyl)benzoic acid (3.00 g, 11.15 mmol, 1.0 equiv.), 4-aminophenol (1.46 g, 13.38 mmol, 1.2 equiv.), K_2CO_3 (4.62 g, 33.46 mmol, 3.0 equiv.), CuO (35 mg, 0.45 mmol, 0.04 equiv.), and Cu (64 mg, 1.00 mmol, 0.09 equiv.) in 2-ethoxyethanol (20 mL).

Yield: 60%; black solid (2 g); ^1H NMR (400 MHz, DMSO) δ 9.69 (s, 1 H), 9.54 (brs, 1 H), 8.08 (d, $J = 1.7$ Hz, 1 H), 7.58 (dd, $J_1 = 9.0$ Hz, $J_2 = 2.2$ Hz, 1 H), 7.14–7.06 (m, 2 H), 6.91 (d, $J = 8.9$ Hz, 1 H), and 6.86–6.79 (m, 2 H).

General procedure for synthesis of methyl ester derivatives **9a–b** (**9a** is given as an example)

2-((4-Hydroxyphenyl)amino)benzoic acid (**8a**) (2.28 g, 9.96 mmol, 1.0 equiv.) was dissolved in anhydrous methanol (100 mL) and then thionyl chloride (11.85 g, 99.59 mmol, 7.22 mL, 10.0 equiv) was slowly added while ice cooling. The batch was stirred overnight at 70 °C. The solvent was removed under reduced pressure, crude product was purified with flash column chromatography using ethyl acetate/hexane = 1:4 as mobile phase and with dry sample loading.

Methyl 2-((4-hydroxyphenyl)amino)benzoate (**9a**): Yield: 55%; white solid (1.33 g); ^1H NMR (400 MHz, DMSO) δ 9.38 (s, 1 H), 9.08 (s, 1 H), 7.85 (dd, $J_1 = 8.0$ Hz, $J_2 = 1.6$ Hz, 1 H), 7.32 (ddd, $J_1 = 8.6$ Hz, $J_2 = 7.2$ Hz, $J_3 = 1.6$ Hz, 1 H), 7.09–7.02 (m, 2 H), 6.86 (dd, $J_1 = 8.6$ Hz, $J_2 = 0.8$ Hz, 1 H), 6.83–6.76 (m, 2 H), 6.67 (ddd, $J = 8.1$ Hz, $J_2 = 7.1$ Hz, $J_3 = 1.1$ Hz, 1 H), and 3.84 (s, 3 H).

Methyl 2-((4-hydroxyphenyl)amino)-5-(trifluoromethyl)benzoate (**9b**): Synthesised from 2-((4-hydroxyphenyl)amino)-5-(trifluoromethyl)benzoic acid (**7b**) (2.00 g, 6.73 mmol, 1.0 equiv.) with thionyl chloride (8.00 g, 67.29 mmol, 4.88 mL, 10.0 equiv.) in anhydrous methanol (75 mL). Purified with flash column chromatography using ethyl acetate/hexane = 1:4 as mobile phase. Yield: 16%; white solid (330 mg); ^1H NMR (400 MHz, DMSO) δ 9.54 (s, 1 H), 9.41 (s, 1 H), 8.09 (d, $J = 1.7$ Hz, 1 H), 7.61 (dd, $J_1 = 9.1$ Hz, $J_2 = 2.2$ Hz, 1 H), 7.10 (d, $J = 8.7$ Hz, 2 H), 6.91 (d, $J = 9.0$ Hz, 1 H), 6.86–6.73 (m, 2 H), and 3.88 (s, 3 H).

General procedure for hydrolysis of methyl ester to obtain **10a–b** (**10a** is given as an example)

Methyl 2-((4-(2-hydroxy-3-morpholinopropoxy)phenyl)amino)benzoate (**5d**) (123 mg, 0.318 mmol, 1.0 equiv.) was dissolved in ethanol (20 mL) and then solution of NaOH (19 mg, 0.477 mmol, 1.5 equiv.) in 1 mL of water was added and stirred at room temperature for 72 h. Solvent was removed under reduced pressure to obtain product **10a**.

2-((4-(2-Hydroxy-3-morpholinopropoxy)phenyl)amino)benzoic acid (**10a**): Yield: 100%; white solid (118 mg); ^1H NMR (400 MHz, DMSO) δ 11.50 (s, 1 H), 7.90 (dd, $J_1 = 7.7$ Hz, $J_2 = 1.6$ Hz, 1 H), 7.11–7.02 (m, 3 H), 6.98 (d, $J = 7.6$ Hz, 1 H), 6.88 (d, $J = 8.9$ Hz, 2 H), 6.62–6.49 (m, 1 H), 4.95 (brs, 1 H), 4.01–3.89 (m, 2 H), 3.88–3.75 (m, 1 H), 3.56 (t, $J = 4.6$ Hz, 4 H), 2.48–2.28 (m, 6 H); ^{13}C NMR (101 MHz, DMSO) δ 171.88, 153.58, 146.66, 135.84, 132.10, 129.92, 122.22, 121.71, 115.62, 115.33, 111.85, 71.34, 66.45, 66.29, 61.60, and 54.09; HRMS (ESI⁺) for C₂₀H₂₅N₂O₅ ([M+H]⁺) calculated 373.1758 found 373.1751; HPLC retention time: 3.033 min (99.37% at 254 nm).

2-((4-(3-(Dimethylamino)-2-hydroxypropoxy)phenyl)amino)-5-(trifluoromethyl)benzoic acid (**10b**): Synthesised from methyl 2-((4-(3-(dimethylamino)-2-hydroxypropoxy)phenyl)amino)-5-(trifluoromethyl)benzoate (**6c**) (28 mg, 0.07 mmol, 1.0 equiv.) with solution of NaOH (4.2 mg, 0.11 mmol, 1.5 equiv.) in 1 mL of water and in ethanol (5 mL) at room temperature for 72 h. Yield: 100%; white solid (28 mg); ^1H NMR (400 MHz, DMSO) δ 12.10 (s, 1 H), 8.16 (d, $J = 2.2$ Hz, 1 H), 7.33 (dd, $J_1 = 8.7$ Hz, $J_2 = 2.3$ Hz, 1 H), 7.10 (d, $J = 8.8$ Hz, 2 H), 6.98 (d, $J = 8.6$ Hz, 1 H), 6.93 (d, $J = 8.9$ Hz, 2 H), 4.87 (brs, 1 H), 4.00–3.77 (m, 3 H), 2.44–2.24 (m, 2 H), 2.18 (s, 6 H). ^{13}C NMR (101 MHz, MeOD) δ 174.97, 157.11, 151.89, 135.41, 130.67 (q, $J = 3.7$ Hz), 128.77 (q, $J = 3.5$ Hz), 126.55 (q, $J = 269.4$ Hz), 125.95, 120.53, 118.11 (q, $J = 32.4$ Hz), 116.51, 112.99, 72.34, 68.80, 63.31, and 46.21; HRMS (ESI⁺) for C₁₉H₂₂F₃N₂O₄ ([M+H]⁺) calculated 399.1526, found 399.1519; HPLC retention time: 3.830 min (95.01% at 254 nm).

1-Chloro-2-nitro-4-(trifluoromethyl)benzene (**11**): resynthesized according to described procedure [26].

General procedure for synthesis of phenol intermediates **12a–d** (**12b** is given as an example)

To a stirred solution of 1-fluoro-2,4-dinitrobenzene (3.00 g, 14.80 mmol, 1.0 equiv.) in acetonitrile (150 mL), NaHCO₃ (3.73 g, 44.40 mmol, 3.0 equiv.) and 4-aminophenol (1.94 g, 17.77 mmol, 1.2 equiv.) were added and the mixture was stirred at 90 °C for 24 h. After reaction mixture was cooled to room temperature and NaHCO₃ was filtered off, the solvent was removed under reduced pressure. The crude product was purified with flash column chromatography using dichloromethane/methanol = 20:1) as eluent and dry sampling loading to obtain **12b**.

4-((2-Nitro-4-(trifluoromethyl)phenyl)amino)phenol (**12a**): resynthesized according to described procedure [26].

4-((2,4-Dinitrophenyl)amino)phenol (**12b**): Yield: 47%; red solid (1.93 g); ¹H NMR (400 MHz, DMSO) δ 10.04 (s, 1 H), 9.73 (s, 1 H), 8.86 (d, *J* = 2.7 Hz, 1 H), 8.17 (dd, *J*₁ = 9.6 Hz, *J*₂ = 2.8 Hz, 1 H), 7.21–7.08 (m, 2 H), 6.94 (d, *J* = 9.6 Hz, 1 H), and 6.91–6.79 (m, 2 H).

2,6-Dibromo-4-((2-nitro-4-(trifluoromethyl)phenyl)amino)phenol (**12c**)

Synthesised from 1-chloro-2-nitro-4-(trifluoromethyl)benzene (**11**) (2.5 g, 11.1 mmol, 1.0 equiv), 4-amino-2,6-dibromophenol (3.55 g, 13.3 mmol, 1.2 equiv), and NaHCO₃ (2 g, 22.2 mmol, 2.0 equiv) in acetonitrile (125 mL) at 90 °C. Purified with flash column chromatography using ethyl acetate/hexane = 1:3 as eluent. Yield: 31%; orange solid (1.59 g); ¹H NMR (400 MHz, CDCl₃) δ 9.51 (s, 1 H), 8.56–8.45 (m, 1 H), 7.59 (dd, *J*₁ = 9.0, *J*₂ = 2.1 Hz, 1 H), 7.49–7.41 (m, 2 H), 7.08 (d, *J* = 9.0 Hz, 1 H), and 5.98 (s, 1 H).

2,6-Dichloro-4-((2-nitro-4-(trifluoromethyl)phenyl)amino)phenol (**12d**)

Synthesised from 1-chloro-2-nitro-4-(trifluoromethyl)benzene (**11**) (2.5 g, 11.1 mmol, 1.0 equiv), 4-amino-2,6-dichlorophenol (2.37 g, 13.3 mmol, 1.2 equiv), and NaHCO₃ (2 g, 22.2 mmol, 2.0 equiv) in acetonitrile (125 mL) at 90 °C. Purified with flash column chromatography using ethyl acetate/hexane = 1:3 as eluent. Yield: 25%; orange solid (1.00 g); ¹H NMR (400 MHz, CDCl₃) δ 9.50 (s, 1 H), 8.61–8.35 (m, 1 H), 7.59 (dd, *J*₁ = 9.0 Hz, *J*₂ = 2.1 Hz, 1 H), 7.26 (s, 2 H), 7.09 (d, *J* = 9.0 Hz, 1 H), and 5.93 (s, 1 H).

N-(4-(2-Morpholinoethoxy)phenyl)-2-nitro-4-(trifluoromethyl)aniline (**13**). To a stirring solution of 4-((2-nitro-4-(trifluoromethyl)phenyl)amino)phenol (**12a**) (300 mg, 1.01 mmol, 1.0 equiv.) in ethanol (30 mL), 4-(2-chloroethyl)morpholine hydrochloride (223 mg, 1.21 mmol, 1.2 equiv.) and KOH (414 mg, 3.03 mmol, 3.0 equiv.) were added to reaction mixture while stirring. The batch was stirred at 100 °C overnight. The next day, solvent was removed under reduced pressure and crude product was purified with flash column chromatography using dichloromethane/methanol/NH₃ = 20:1:0.01 as eluent. Yield: 29%; red solid (120 mg); R_f (dichloromethane/methanol = 20:1) = 0.55; ¹H NMR (400 MHz, CDCl₃) δ 9.61 (s, 1 H), 8.50 (d, *J* = 1.1 Hz, 1 H), 7.49 (dd, *J*₁ = 9.1 Hz, *J*₂ = 2.1 Hz, 1 H), 7.22–7.15 (m, 2 H), 7.05 (d, *J* = 9.1 Hz, 1 H), 7.02–6.96 (m, 2 H), 4.15 (t, *J* = 5.7 Hz, 2 H), 3.84–3.68 (m, 4 H), 2.84 (t, *J* = 5.7 Hz, 2 H), 2.66–2.53 (m, 4 H); ¹³C NMR (101 MHz, CDCl₃) δ 157.90, 146.45, 131.84 (q, *J* = 3.0 Hz), 131.47, 130.32, 127.56, 124.88 (q, *J* = 4.5 Hz), 123.60 (q, *J* = 271.2 Hz), 118.96 (q, *J* = 34.4 Hz), 116.62, 116.03, 67.08, 66.34, 57.73, and 54.27; HRMS (ESI⁺) for C₁₉H₂₁F₃N₃O₄ ([M+H]⁺) calculated 412.1479 found 412.1473; HPLC retention time: 4.247 min (99.01% at 254 nm).

N-(4-(Benzyloxy)phenyl)-2-nitro-4-(trifluoromethyl)aniline (**14**): To a stirring solution of 4-((2-nitro-4-(trifluoromethyl)phenyl)amino)phenol (**12a**) (200 mg, 0.8 mmol, 1.0 equiv.) in toluene (50 mL), NaHCO₃ (134 mg, 1.6 mmol, 2.0 equiv) and 4-benzyloxy aniline were added (150 mg, 1.6 mmol, 2.0 equiv.). The batch was stirred at 100 °C for 24 h. Solvent was removed under reduced pressure and crude product was purified with Biotage Isolera One System reversed-phase chromatography (Biotage SNAP Cartridge KP-C18-HS 12 g column), MF: gradient water in H₂O/acetonitrile. Yield: 31%; red solid (95 mg); ¹H NMR (400 MHz, CDCl₃) δ 9.61 (s, 1 H), 8.50 (s, 1 H), 7.53–7.32 (m, 6 H), 7.19 (d, *J* = 8.8 Hz, 2 H), 7.06 (d, *J* = 8.9 Hz, 3 H), 5.11 (s, 2 H); ¹³C NMR (101 MHz, CDCl₃) δ ¹³C NMR (101 MHz, CDCl₃) δ 157.92, 146.43, 136.65, 131.83 (q, *J* = 3.0 Hz), 131.47, 130.38, 128.84, 128.34, 127.63, 127.56, 124.87 (q, *J* = 4.3 Hz), 123.65 (q, *J* = 268.0 Hz), 118.95 (q, *J* = 34.4 Hz), 116.65, 116.33, and 70.50; HRMS (ESI⁻) for C₂₀H₁₄F₃N₂O₃ ([M]⁻) calculated 387.0962 found 387.0964; HPLC retention time: 7.033 min (99.77% at 254 nm).

1-(Methylamino)-3-(4-((2-nitro-4-(trifluoromethyl)phenyl)amino)phenoxy)propan-2-ol (**15**): To a stirring solution of 2-nitro-*N*-(4-(oxiran-2-ylmethoxy)phenyl)-4-(trifluoromethyl)aniline (**4f**) (500 mg, 1.41 mmol, 1.0 equiv.) in acetonitrile (50 mL), MeNH₂ (263 mg, 8.47 mmol, 6.0 equiv.) and K₂CO₃ (581 mg, 4.23 mmol, 3.0 equiv.) were added. The batch was stirred at 70 °C for 24 h. Solvent was removed under reduced pressure and crude product was purified with flash column chromatography using dichloromethane/methanol/NH₃ = 20:1:0 as mobile phase. Yield: 22%; red solid (120 mg); ¹H NMR (400 MHz, DMSO) δ 9.73 (s, 1 H), 8.35 (d, *J* = 1.3 Hz, 1 H), 7.72 (dd, *J*₁ = 9.2 Hz, *J*₂ = 2.2 Hz, 1 H), 7.35–7.20 (m, 2 H), 7.10–6.95 (m, 3 H), 3.99 (q, *J* = 7.0 Hz, 1 H), 3.91 (t, *J* = 5.9 Hz, 2 H), 2.69–2.51 (m, 2 H), 2.31 (s, 3 H). ¹³C NMR (101 MHz, CDCl₃) δ 157.84, 146.41, 131.85 (q, *J* = 2.9 Hz), 131.46, 130.46, 127.56, 124.86 (q, *J* = 4.9 Hz), 123.54 (q, *J* = 270.0 Hz), 118.95 (q, *J* = 34.4 Hz), 116.61, 116.01, 73.35, 70.99, 68.10, 63.07, 53.98, 47.99, 36.48, and 31.09; HRMS (ESI⁺) for C₁₇H₁₉F₃N₃O₄ ([M+H]⁺) calculated 386.1322 found 386.1318; HPLC retention time: 4.063 min (95.47% at 254 nm).

General procedure for opening of the epoxide with various aromatic amines to obtain **16a–d** (**16a** is given as example)

To a stirring solution of 2-nitro-*N*-(4-(oxiran-2-ylmethoxy)phenyl)-4-(trifluoromethyl)aniline (**4f**) (100 mg, 0.28 mmol, 1.0 equiv.) in acetonitrile (20 mL), 4-((3,4-dichlorophenoxy)methyl)piperidin-4-ol (78 mg, 0.28 mmol, 1.0 equiv.) was added. The batch was stirred for 24 h at 70 °C. The next day, solvent was removed under reduced pressure and crude product was purified with flash column chromatography using dichloromethane/methanol = 100:1.

4-((3,4-Dichlorophenoxy)methyl)-1-(2-hydroxy-3-(4-((2-nitro-4-(trifluoromethyl)phenyl)amino)phenoxy)propyl)piperidin-4-ol (**16a**): Yield: 17%; red solid (30 mg); ¹H NMR (400 MHz, CDCl₃) δ 9.61 (s, 1 H), 8.49 (d, *J* = 1.0 Hz, 1 H), 7.49 (dd, *J*₁ = 9.1 Hz, *J*₂ = 2.0 Hz, 1 H), 7.34 (d, *J* = 8.9 Hz, 1 H), 7.19 (t, *J* = 5.9 Hz, 2 H), 7.11–6.95 (m, 4 H), 6.79 (dd, *J*₁ = 8.9 Hz, *J*₂ = 2.9 Hz, 1 H), 4.16 (td, *J*₁ = 9.3 Hz, *J*₂ = 4.8 Hz, 1 H), 4.09–3.97 (m, 2 H), 3.81 (s, 2 H), 2.87 (d, *J* = 11.3 Hz, 1 H), 2.83–2.57 (m, 4 H), 2.51 (td, *J*₁ = 11.3 Hz, *J*₂ = 3.0 Hz, 1 H), 1.92–1.66 (m, 4 H); ¹³C NMR (101 MHz, CDCl₃) δ 157.90, 157.71, 146.39, 133.09, 131.82 (q, *J* = 3.0 Hz), 131.42, 130.90, 130.41, 127.51, 124.82 (q, *J* = 4.2 Hz), 124.69, 123.58 (q, *J* = 271.0 Hz), 118.90 (q, *J* = 34.4 Hz), 116.62, 116.60, 116.00, 114.67, 76.24, 70.79, 68.80, 65.64, 60.50, 50.41, 47.90, 34.21, and 34.00; HRMS (ESI⁺) for C₂₈H₂₉Cl₂F₃N₃O₆ ([M+H]⁺) calculated 630.1380 found 630.1365; HPLC retention time: 5.577 min (98.11% at 254 nm).

1-(2-Hydroxy-3-(4-((2-nitro-4-(trifluoromethyl)phenyl)amino)phenoxy)propyl)-4-((4-methoxyphenoxy)methyl)piperidin-4-ol (**16b**): Synthesised from 2-nitro-*N*-(4-(oxiran-2-ylmethoxy)phenyl)-4-(trifluoromethyl)aniline (**4f**) (100 mg, 0.282 mmol, 1.0 equiv.) and 4-((4-methoxyphenoxy)methyl)piperidin-4-ol (67 mg, 0.282 mmol, 1.0 equiv.) in acetonitrile (20 mL). Purified with flash column chromatography using dichloromethane/methanol = 100:1. Yield: 14%; red solid (23 mg); ¹H NMR (400 MHz, CDCl₃) δ 9.60 (s, 1 H), 8.49 (d, *J* = 1.1 Hz, 1 H), 7.49 (dd, *J*₁ = 9.1 Hz, *J*₂ = 2.1 Hz, 1 H), 7.18 (t, *J* = 6.0 Hz, 2 H), 7.08–6.96 (m, 3 H), 6.92–6.77 (m, 4 H), 4.23–4.12 (m, 1 H), 4.10–3.97 (m, 2 H), 3.78 (s, 2 H), 3.77 (s, 3 H), 2.91–2.75 (m, 2 H), 2.74–2.57 (m, 3 H), 2.52 (td, *J*₁ = 11.3 Hz, *J*₂ = 2.9 Hz, 1 H), 1.88–1.67 (m, 4 H); ¹³C NMR (101 MHz, CDCl₃) δ 157.92, 154.30, 152.87, 146.40, 131.80 (q, *J* = 2.9 Hz), 131.41, 130.37, 127.50, 124.81 (q, *J* = 4.2 Hz), 123.58 (q, *J* = 270.9 Hz), 118.87 (q, *J* = 34.3 Hz), 116.60, 116.00, 115.68, 114.81, 76.43, 70.82, 68.85, 65.60, 60.52, 55.83, 50.55, 48.06, 34.29, and 34.08; HRMS (ESI⁺) for C₂₉H₃₃F₃N₃O₇ ([M+H]⁺) calculated 592.2265 found 592.2251; HPLC retention time: 5.073 min (97.04% at 254 nm).

3,4-Dichloro-*N*-(1-(2-hydroxy-3-(4-((2-nitro-4-(trifluoromethyl)phenyl)amino)phenoxy)propyl)piperidin-4-yl)benzamide (**16c**): Synthesised from 2-nitro-*N*-(4-(oxiran-2-ylmethoxy)phenyl)-4-(trifluoromethyl)aniline (**4f**) (100 mg, 0.282 mmol, 1.0 equiv.) and 3,4-dichloro-*N*-(piperidin-4-yl)benzamide (77 mg, 0.282 mmol, 1.0 equiv.) in acetonitrile (20 mL). Purified with flash column chromatography using dichloromethane/methanol = 100:1. Yield: 17%; red solid (30 mg); ¹H NMR (400 MHz, CDCl₃) δ 9.60 (s, 1 H), 8.50 (d, *J* = 1.1 Hz, 1 H), 7.85 (d, *J* = 2.0 Hz, 1 H), 7.59 (dd, *J*₁ = 8.3 Hz, *J*₂ = 2.0 Hz, 1 H), 7.54–7.46 (m, 2 H), 7.24–7.16 (m, 2 H), 7.08–6.96 (m, 3 H), 6.07 (d, *J* = 7.7 Hz, 1 H), 4.13 (td, *J*₁ = 9.3 Hz, *J*₂ = 4.4 Hz, 1 H), 4.09–3.96 (m, 3 H), 3.07 (d, *J* = 11.6 Hz, 1 H), 2.90 (d, *J* = 11.7 Hz, 1 H), 2.70–2.48 (m, 3 H),

2.29–2.19 (m, 1 H), 2.09 (d, $J = 11.2$ Hz, 2 H), 1.72–1.50 (m, 2 H); ^{13}C NMR (101 MHz, CDCl_3) δ 164.84, 157.85, 146.40, 136.06, 134.53, 133.21, 131.85 (q, $J = 2.9$ Hz), 131.47, 130.77, 130.47, 129.25, 127.54, 126.21, 124.87 (q, $J = 4.6$ Hz), 123.59 (q, $J = 271.1$ Hz), 118.97 (q, $J = 34.4$ Hz), 116.60, 115.99, 70.67, 65.74, 60.36, 54.15, 51.34, 47.40, 32.63, and 32.33; HRMS (ESI⁺) for $\text{C}_{28}\text{H}_{28}\text{Cl}_2\text{F}_3\text{N}_4\text{O}_5$ ($[\text{M}+\text{H}]^+$) calculated 627.1383 found 627.1369; HPLC retention time: 5.313 min (99.57% at 254 nm).

2-(3,4-Dichlorophenyl)-*N*-(1-(2-hydroxy-3-(4-((2-nitro-4-(trifluoromethyl)phenyl)amino)phenoxy)propyl)piperidin-4-yl)acetamide (**16d**): Synthesised from 2-nitro-*N*-(4-(oxiran-2-ylmethoxy)phenyl)-4-(trifluoromethyl)aniline (**4f**) (100 mg, 0.282 mmol, 1.0 equiv.) and 2-(3,4-dichlorophenyl)-*N*-(piperidin-4-yl)acetamide (81 mg, 0.282 mmol, 1.0 equiv) in acetonitrile (20 mL). Purified with flash column chromatography using dichloromethane/methanol = 100:1. Yield: 22%; red solid (40 mg); ^1H NMR (400 MHz, DMSO) δ 9.74 (s, 1 H), 8.35 (d, $J = 1.3$ Hz, 1 H), 8.04 (d, $J = 7.6$ Hz, 1 H), 7.72 (dd, $J_1 = 9.2$ Hz, $J_2 = 2.2$ Hz, 1 H), 7.55 (d, $J = 8.2$ Hz, 1 H), 7.50 (d, $J = 2.0$ Hz, 1 H), 7.31–7.25 (m, 2 H), 7.22 (dd, $J_1 = 8.3$ Hz, $J_2 = 2.0$ Hz, 1 H), 7.13–6.98 (m, 3 H), 4.87 (d, $J = 4.2$ Hz, 1 H), 4.01 (dd, $J = 9.2, 3.1$ Hz, 1 H), 3.98–3.85 (m, 1 H), 3.56–3.44 (m, 1 H), 3.41 (s, 1 H), 2.91–2.77 (m, 1 H), 2.40 (ddd, $J = 33.4, 12.7, 5.9$ Hz, 1 H), 2.08 (dd, $J = 19.9, 9.4$ Hz, 1 H), 1.76–1.63 (m, 1 H), 1.39 (dd, $J = 21.8, 10.8$ Hz, 1 H); ^{13}C NMR (101 MHz, CDCl_3) δ 169.14, 157.87, 146.40, 135.13, 132.98, 131.84 (q, $J = 2.9$ Hz), 131.68, 131.45, 131.31, 130.91, 130.44, 128.74, 127.54, 124.86 (q, $J = 4.7$ Hz), 123.55 (q, $J = 277.7$ Hz), 118.96 (q, $J = 34.5$ Hz), 116.60, 116.00, 70.69, 65.69, 60.32, 54.02, 51.25, 46.90, 42.85, 32.50, and 32.21; HRMS (ESI⁺) for $\text{C}_{29}\text{H}_{29}\text{Cl}_2\text{F}_3\text{N}_4\text{O}_5$ ($[\text{M}+\text{H}]^+$) calculated 641.1540 found 641.1524; HPLC retention time: 5.280 min (97.83% at 254 nm).

General procedure for synthesis of (diethylamino)ethoxy compounds **17a–c** (**17a** is given as example)

To a stirring solution of 4-((2-nitro-4-(trifluoromethyl)phenyl)amino)phenol (**12a**) (300 mg, 1.00 mmol, 1.0 equiv.) in ethanol (30 mL), 2-chloro-*N,N*-diethylethan-1-amine hydrochloride (206 mg, 1.2 mmol, 1.2 equiv) and KOH (414 mg, 7.38 mmol, 7.3 equiv) were added. Batch was stirred overnight at 100 °C. KOH was filtered off and solvent was removed under reduced pressure. Crude product was purified with flash column chromatography using dichloromethane/methanol/ $\text{NH}_3 = 10:1:0.01$ and dry sample loading.

N-(4-(2-(Diethylamino)ethoxy)phenyl)-2-nitro-4-(trifluoromethyl)aniline (**17a**): Yield: 38%; red solid (150 mg); ^1H NMR (400 MHz, CDCl_3) δ 9.60 (s, 1 H), 8.49 (d, $J = 1.3$ Hz, 1 H), 7.48 (dd, $J_1 = 9.1$ Hz, $J_2 = 2.1$ Hz, 1 H), 7.20–7.14 (m, 2 H), 7.04 (d, $J = 9.1$ Hz, 1 H), 7.01–6.95 (m, 2 H), 4.07 (t, $J = 6.3$ Hz, 2 H), 2.90 (t, $J = 6.3$ Hz, 2 H), 2.66 (q, $J = 7.1$ Hz, 4 H), 1.09 (t, $J = 7.1$ Hz, 6 H); ^{13}C NMR (101 MHz, CDCl_3) δ 158.11, 146.52, 131.82 (q, $J = 3.0$ Hz), 131.41, 130.06, 127.54, 124.86 (q, $J = 4.3$ Hz), 123.62 (q, $J = 270.8$ Hz), 118.87 (q, $J = 34.4$ Hz), 116.65, 115.96, 67.20, 51.87, 48.05, and 12.01; HRMS (ESI⁺) for $\text{C}_{19}\text{H}_{22}\text{F}_3\text{N}_3\text{O}_3$ ($[\text{M}+\text{H}]^+$) calculated 398.1686 found 398.1682; HPLC retention time: 4.323 min (98.90% at 254 nm).

3,5-Dibromo-4-(2-(diethylamino)ethoxy)-*N*-(2-nitro-4-(trifluoromethyl)phenyl)aniline (**17b**): Synthesised from 2,6-dibromo-4-((2-nitro-4-(trifluoromethyl)phenyl)amino)phenol (**12c**) (300 mg, 0.66 mmol, 1.0 equiv), 2-chloro-*N,N*-diethylethan-1-amine hydrochloride (227 mg, 1.32 mmol, 2.0 equiv), and K_2CO_3 (273 mg, 2.0 mmol, 3.0 equiv) at 90 °C in acetonitrile (40 mL) overnight. Purified with flash column chromatography using ethyl acetate/hexane = 1:1 as eluent and dry sample loading. Yield: 15%; orange solid (55 mg); ^1H NMR (400 MHz, CDCl_3) δ 9.53 (s, 1 H), 8.49 (d, $J = 1.4$ Hz, 1 H), 7.63 (dd, $J_1 = 9.0$ Hz, $J_2 = 2.0$ Hz, 1 H), 7.48 (s, 2 H), 7.21 (d, $J = 9.0$ Hz, 1 H), 4.37 (t, $J = 5.0$ Hz, 2 H), 3.54 (t, $J = 9.2$ Hz, 2 H), 3.29 (q, $J = 6.8$ Hz, 4 H), 1.36 (t, $J = 7.2$ Hz, 6 H); ^{13}C NMR (101 MHz, CDCl_3) δ 151.00, 144.11, 136.23, 132.75, 132.30 (q, $J = 3.1$ Hz), 129.08, 124.88 (q, $J = 4.1$ Hz), 123.25 (q, $J = 271.8$ Hz), 120.85 (q, $J = 34.6$ Hz), 119.20, 116.58, 68.46, 50.73, 47.52, and 9.53; HRMS (ESI⁺) for $\text{C}_{19}\text{H}_{20}\text{Br}_2\text{F}_3\text{N}_3\text{O}_3$ ($[\text{M}+\text{H}]^+$) calculated 553.9896 found 553.9894; HPLC retention time: 4.717 min (95.89% at 254 nm).

3,5-Dichloro-4-(2-(diethylamino)ethoxy)-*N*-(2-nitro-4-(trifluoromethyl)phenyl)aniline (**17c**): Synthesised from 2,6-dichloro-4-((2-nitro-4-(trifluoromethyl)phenyl)amino)phenol (**12d**) (240 mg, 0.65 mmol, 1.0 equiv), 2-chloro-*N,N*-diethylethan-1-amine hydrochloride

(190 mg, 1.3 mmol, 2.0 equiv), and K_2CO_3 (271 mg, 2.0 mmol, 3.0 equiv.) at 90 °C in acetonitrile (40 mL) overnight. Purified with flash column chromatography using ethyl acetate/hexane = 1:1 as eluent and dry sample loading. Yield: 15%; orange solid (40 mg); 1H NMR (400 MHz, $CDCl_3$) δ 9.53 (s, 1 H), 8.51 (d, J = 1.3 Hz, 1 H), 7.62 (dd, J_1 = 9.0 Hz, J_2 = 2.1 Hz, 1 H), 7.26 (s, 2 H), 7.21 (d, J = 9.0 Hz, 1 H), 4.14 (t, J = 6.5 Hz, 2 H), 3.00 (t, J = 6.5 Hz, 2 H), 2.69 (q, J = 7.1 Hz, 4 H), 1.09 (t, J = 7.1 Hz, 6 H); ^{13}C NMR (101 MHz, $CDCl_3$) δ 150.59, 144.51, 134.30, 132.56, 132.27 (q, J = 3.0 Hz), 130.74, 125.63, 124.95 (q, J = 4.1 Hz), 123.35 (q, J = 271.5 Hz), 120.58 (q, J = 34.6 Hz), 116.63, 72.00, 52.37, 47.64, and 11.87; HRMS (ESI⁺) for $C_{19}H_{20}Cl_2F_3N_3O_3$ ([M+H]⁺) calculated 466.0903 found 466.0907; HPLC retention time: 4.603 min (95.04% at 254 nm).

General procedure for synthesis of (dimethylamino)ethoxy compounds **18a–c** (**18a** is given as an example)

To a stirring solution of 4-((2-nitro-4-(trifluoromethyl)phenyl)amino)phenol (**12a**) (300 mg, 1.01 mmol, 1.0 equiv.) in ethanol (30 mL), 2-chloro-*N,N*-dimethylethan-1-amine hydrochloride (174 mg, 1.21 mmol) and KOH (414 mg, 7.38 mmol, 7.3 equiv.) were added. Batch was stirred overnight at 100 °C. Solvent was removed under reduced pressure and product was purified with flash column chromatography using dichloromethane/methanol/ NH_3 = 10:1:0.01 and dry sample loading.

N-(4-(2-(Dimethylamino)ethoxy)phenyl)-2-nitro-4-(trifluoromethyl)aniline (**18a**): Yield: 27%; red solid (100 mg); R_f (dichloromethane/methanol = 20:1) = 0.05; 1H NMR (400 MHz, $CDCl_3$) δ 9.61 (s, 1 H), 8.50 (d, J = 1.1 Hz, 1 H), 7.49 (dd, J_1 = 9.1 Hz, J_2 = 2.1 Hz, 1 H), 7.22–7.14 (m, 2 H), 7.08–6.96 (m, 3 H), 4.11 (t, J = 5.7 Hz, 2 H), 2.78 (t, J = 5.7 Hz, 2 H), 2.38 (s, 6 H); ^{13}C NMR (101 MHz, $CDCl_3$) δ 158.01, 146.48, 131.83 (q, J = 3.1 Hz), 131.42, 130.19, 127.52, 124.85 (q, J = 4.3 Hz), 123.61 (q, J = 271.0 Hz), 118.89 (q, J = 34.4 Hz), 116.65, 116.00, 66.46, 58.37, and 46.05; HRMS (ESI⁺) for $C_{17}H_{19}F_3N_3O_3$ ([M+H]⁺) calculated 370.1373 found 370.1368; HPLC retention time: 4.200 min (97.85% at 254 nm).

3,5-Dibromo-4-(2-(dimethylamino)ethoxy)-*N*-(2-nitro-4-(trifluoromethyl)phenyl)aniline (**18b**): Synthesised from 2,6-dibromo-4-((2-nitro-4-(trifluoromethyl)phenyl)amino)phenol (**12c**) (300 mg, 0.66 mmol, 1.0 equiv), 2-chloro-*N,N*-dimethylethan-1-amine hydrochloride (112 mg, 0.8 mmol, 1.2 equiv) and K_2CO_3 (273 mg, 2.0 mmol, 3.0 equiv) in acetonitrile (40 mL) at 90 °C overnight. Purified with flash column chromatography using flash column chromatography using ethyl acetate/hexane = 1:1 as eluent and dry sample loading. Yield: 17%; orange solid (60 mg); 1H NMR (400 MHz, $CDCl_3$) δ 9.54 (s, 1 H), 8.51 (d, J = 1.3 Hz, 1 H), 7.62 (dd, J_1 = 9.0 Hz, J_2 = 2.0 Hz, 1 H), 7.47 (s, 2 H), 7.20 (d, J = 9.0 Hz, 1 H), 4.14 (t, J = 5.9 Hz, 2 H), 2.85 (t, J = 5.9 Hz, 2 H), 2.39 (s, 6 H); ^{13}C NMR (101 MHz, $CDCl_3$) δ 152.41, 144.49, 135.27, 132.54, 132.27 (q, J = 3.1 Hz), 129.30, 124.93 (q, J = 4.1 Hz), 123.34 (d, J = 271.2 Hz), 120.59 (q, J = 34.6 Hz), 119.31, 116.61, 71.35, 58.87, and 46.00; HRMS (ESI⁺) for $C_{17}H_{16}Br_2F_3N_3O_3$ ([M+H]⁺) calculated 525.9583 found 525.9580; HPLC retention time: 4.417 min (99.88% at 254 nm).

3,5-Dichloro-4-(2-(dimethylamino)ethoxy)-*N*-(2-nitro-4-(trifluoromethyl)phenyl)aniline (**18c**): Synthesised from 2,6-dichloro-4-((2-nitro-4-(trifluoromethyl)phenyl)amino)phenol (**12d**) (300 mg, 0.82 mmol, 1.0 equiv), 2-chloro-*N,N*-dimethylethan-1-amine hydrochloride (235 mg, 1.6 mmol, 2.0 equiv), and K_2CO_3 (338 mg, 2.45 mmol, 3.0 equiv) in acetonitrile (40 mL) at 90 °C overnight. Purified with flash column chromatography using ethyl acetate/hexane = 1:1 as eluent and dry sample loading. Yield: 16%; orange solid (57 mg); 1H NMR (400 MHz, $CDCl_3$) δ 9.53 (s, 1 H), 8.51 (d, J = 1.4 Hz, 1 H), 7.62 (dd, J_1 = 9.0 Hz, J_2 = 2.1 Hz, 1 H), 7.26 (s, 2 H), 7.21 (d, J = 9.0 Hz, 1 H), 4.15 (t, J = 5.8 Hz, 2 H), 2.82 (t, J = 5.8 Hz, 2 H), 2.38 (s, 6 H); ^{13}C NMR (101 MHz, $CDCl_3$) δ 150.46, 144.45, 134.38, 132.55, 132.24 (q, J = 3.1 Hz), 130.76, 125.57, 124.92 (q, J = 4.2 Hz), 123.33 (q, J = 271.3 Hz), 120.56 (q, J = 34.6 Hz), 116.63, 71.51, 58.89, and 45.93; HRMS (ESI⁺) for $C_{17}H_{16}Cl_2F_3N_3O_3$ ([M+H]⁺) calculated 438.0594 found 438.0591; HPLC retention time: 4.307 min (98.68% at 254 nm).

2-Nitro-*N*-(4-(2-(pyrrolidin-1-yl)ethoxy)phenyl)-4-(trifluoromethyl)aniline (**19**): To a stirring solution of 4-((2-nitro-4-(trifluoromethyl)phenyl)amino)phenol (**12a**) (300 mg, 1.00 mmol, 1.0 equiv.) in acetonitrile (40 mL), 1-(2-chloroethyl)pyrrolidine \times HCl (204 mg,

1.2 mmol, 1.2 equiv) and K_2CO_3 (414 mg, 3.0 mmol, 3.0 equiv) were added. Batch was stirred overnight at 90 °C. K_2CO_3 was filtered off and solvent was removed under reduced pressure. Crude product was purified with flash column chromatography using dichloromethane/methanol = 40:1 and dry sample loading. Yield: 30%; red solid (120 mg); 1H NMR (400 MHz, $CDCl_3$) δ 9.60 (s, 1 H), 8.49 (d, J = 1.6 Hz, 1 H), 7.48 (dd, J_1 = 9.1 Hz, J_2 = 2.1 Hz, 1 H), 7.21–7.13 (m, 2 H), 7.04 (d, J = 9.1 Hz, 1 H), 7.02–6.93 (m, 2 H), 4.15 (t, J = 5.9 Hz, 2 H), 2.95 (t, J = 5.9 Hz, 2 H), 2.67 (t, J = 6.6 Hz, 4 H), 1.84 (h, J = 3.2 Hz, 4 H); ^{13}C NMR (101 MHz, $CDCl_3$) δ 158.00, 146.47, 131.81 (q, J = 3.1 Hz), 131.40, 130.14, 127.52, 124.93 (d, J = 271.6 Hz), 124.83 (q, J = 4.3 Hz), 118.86 (q, J = 34.4 Hz), 116.64, 116.00, 67.52, 55.14, 54.90, and 23.63; HRMS (ESI⁺) for $C_{19}H_{20}F_3N_3O_3$ ([M+H]⁺) calculated 396.15295 found 396.15260; HPLC retention time: 4.190 min (98.91% at 254 nm).

2-Nitro-*N*-(4-(2-(piperidin-1-yl)ethoxy)phenyl)-4-(trifluoromethyl)aniline (**20**): To a stirring solution of 4-((2-nitro-4-(trifluoromethyl)phenyl)amino)phenol (**12a**) (300 mg, 1.00 mmol, 1.0 equiv.) in acetonitrile (40 mL), 1-(2-chloroethyl)piperidine \times HCl (370 mg, 2.0 mmol, 2.0 equiv) and K_2CO_3 (414 mg, 3.0 mmol, 3.0 equiv) were added. Batch was stirred overnight at 90 °C. K_2CO_3 was filtered off and solvent was removed under reduced pressure. Crude product was purified with flash column chromatography using ethyl acetate/hexane = 1:1 as eluent and dry sample loading. Yield: 27%; red solid (109 mg); 1H NMR (400 MHz, $CDCl_3$) δ 9.60 (s, 1 H), 8.49 (d, J = 1.3 Hz, 1 H), 7.48 (dd, J_1 = 9.1 Hz, J_2 = 2.2 Hz, 1 H), 7.22–7.13 (m, 2 H), 7.04 (d, J = 9.1 Hz, 1 H), 7.01–6.94 (m, 2 H), 4.13 (t, J = 6.0 Hz, 2 H), 2.79 (t, J = 6.0 Hz, 2 H), 2.52 (s, 4 H), 1.62 (p, J = 5.6 Hz, 4 H), 1.46 (q, J = 5.9 Hz, 2 H); ^{13}C NMR (101 MHz, $CDCl_3$) δ 158.04, 146.49, 131.81 (q, J = 3.1 Hz), 131.41, 130.11, 127.52, 124.85 (q, J = 4.3 Hz), 123.61 (q, J = 271.0 Hz), 118.88 (q, J = 34.4 Hz), 116.65, 116.02, 66.53, 58.03, 55.26, 26.09, and 24.32; HRMS (ESI⁺) for $C_{20}H_{22}F_3N_3O_3$ ([M+H]⁺) calculated 410.1686 found 410.1682; HPLC retention time: 4.283 min (99.95% at 254 nm).

N-(4-(2-(Azepan-1-yl)ethoxy)phenyl)-2-nitro-4-(trifluoromethyl)aniline (**21**): To a stirring solution of 4-((2-nitro-4-(trifluoromethyl)phenyl)amino)phenol (**12a**) (300 mg, 1.00 mmol, 1.0 equiv.) in acetonitrile (40 mL), 1-(2-chloroethyl)azepane hydrochloride \times HCl (400 mg, 2.0 mmol, 2.0 equiv) and K_2CO_3 (414 mg, 3.0 mmol, 3.0 equiv) were added. Batch was stirred overnight at 90 °C. K_2CO_3 was filtered off and solvent was removed under reduced pressure. Crude product was purified with flash column chromatography using ethyl acetate/hexane = 1:1 as eluent and dry sample loading. Yield: 26%; red solid (112 mg); 1H NMR (400 MHz, $CDCl_3$) δ 9.60 (s, 1 H), 8.49 (d, J = 1.4 Hz, 1 H), 7.48 (dd, J_1 = 9.1 Hz, J_2 = 2.1 Hz, 1 H), 7.21–7.15 (m, 2 H), 7.04 (d, J = 9.1 Hz, 1 H), 7.01–6.96 (m, 2 H), 4.09 (t, J = 6.2 Hz, 2 H), 2.98 (t, J = 6.2 Hz, 2 H), 2.84–2.74 (m, 4 H), 1.75–1.57 (m, 8 H); ^{13}C NMR (101 MHz, $CDCl_3$) δ 158.14, 146.51, 131.81 (q, J = 3.0 Hz), 131.41, 130.05, 127.52, 124.85 (q, J = 4.3 Hz), 123.61 (q, J = 271.0 Hz), 118.87 (q, J = 34.4 Hz), 116.65, 116.02, 67.09, 56.41, 56.05, 28.10, and 27.21; HRMS (ESI⁺) for $C_{21}H_{24}F_3N_3O_3$ ([M+H]⁺) calculated 424.1843 found 424.1837; HPLC retention time: 4.450 min (99.58% at 254 nm).

References

1. Drysdale, R.; Warmke, J.; Kreber, R.; Ganetzky, B. Molecular Characterization of Eag: A Gene Affecting Potassium Channels in *Drosophila Melanogaster*. *Genetics* **1991**, *127*, 497–505. [[CrossRef](#)] [[PubMed](#)]
2. Lin, T.-F.; Jow, G.-M.; Fang, H.-Y.; Fu, S.-J.; Wu, H.-H.; Chiu, M.-M.; Jeng, C.-J. The Eag Domain Regulates the Voltage-Dependent Inactivation of Rat Eag1 K⁺ Channels. *PLoS ONE* **2014**, *9*, e110423. [[CrossRef](#)]
3. Whicher, J.R.; MacKinnon, R. Structure of the Voltage-Gated K⁺ Channel Eag1 Reveals an Alternative Voltage Sensing Mechanism. *Science* **2016**, *353*, 664–669. [[CrossRef](#)] [[PubMed](#)]
4. Pardo, L.A.; del Camino, D.; Sánchez, A.; Alves, F.; Brüggemann, A.; Beckh, S.; Stühmer, W. Oncogenic Potential of EAG K(+) Channels. *EMBO J.* **1999**, *18*, 5540–5547. [[CrossRef](#)] [[PubMed](#)]
5. Hemmerlein, B.; Weseloh, R.M.; Mello de Queiroz, F.; Knötgen, H.; Sánchez, A.; Rubio, M.E.; Martin, S.; Schliephacke, T.; Jenke, M.; Heinz-Joachim-Radzun; et al. Overexpression of Eag1 Potassium Channels in Clinical Tumours. *Mol. Cancer* **2006**, *5*, 41. [[CrossRef](#)] [[PubMed](#)]
6. Pardo, L.A.; Gomez-Varela, D.; Major, F.; Sansuk, K.; Leurs, R.; Downie, B.R.; Tietze, L.F.; Stühmer, W. Approaches Targeting Kv10.1 Open a Novel Window for Cancer Diagnosis and Therapy. *Curr. Med. Chem.* **2012**, *19*, 675–682. [[CrossRef](#)] [[PubMed](#)]
7. Pardo, L.A.; Stühmer, W. The Roles of K⁺ Channels in Cancer. *Nat. Rev. Cancer* **2014**, *14*, 39–48. [[CrossRef](#)]

8. Movsisyan, N.; Pardo, L.A. Kv10.1 Regulates Microtubule Dynamics during Mitosis. *Cancers* **2020**, *12*, 2409. [[CrossRef](#)]
9. García-Quiroz, J.; García-Becerra, R.; Santos-Martínez, N.; Barrera, D.; Ordaz-Rosado, D.; Avila, E.; Halhali, A.; Villanueva, O.; Ibarra-Sánchez, M.J.; Esparza-López, J.; et al. In Vivo Dual Targeting of the Oncogenic Ether-à-Go-Go-1 Potassium Channel by Calcitriol and Astemizole Results in Enhanced Antineoplastic Effects in Breast Tumors. *BMC Cancer* **2014**, *14*, 745. [[CrossRef](#)]
10. Bai, Y.; Liao, H.; Liu, T.; Zeng, X.; Xiao, F.; Luo, L.; Guo, H.; Guo, L. MiR-296-3p Regulates Cell Growth and Multi-Drug Resistance of Human Glioblastoma by Targeting Ether-à-Go-Go (EAG1). *Eur. J. Cancer* **2013**, *49*, 710–724. [[CrossRef](#)]
11. Wu, J.; Wu, X.; Zhong, D.; Zhai, W.; Ding, Z.; Zhou, Y. Short Hairpin Rna (ShRNA) Ether à Go-Go 1 (Eag1) Inhibition of Human Osteosarcoma Angiogenesis via VEGF/PI3K/AKT Signaling. *Int. J. Mol. Sci.* **2012**, *13*, 12573–12583. [[CrossRef](#)]
12. Wang, X.; Chen, Y.; Li, J.; Guo, S.; Lin, X.; Zhang, H.; Zhan, Y.; An, H. Tetrandrine, a Novel Inhibitor of Ether-à-Go-Go-1 (Eag1), Targeted to Cervical Cancer Development. *J. Cell. Physiol.* **2018**, *234*, 7161–7173. [[CrossRef](#)]
13. Gómez-Varela, D.; Zwick-Wallasch, E.; Knötgen, H.; Sánchez, A.; Hettmann, T.; Ossipov, D.; Weseloh, R.; Contreras-Jurado, C.; Rothe, M.; Stühmer, W.; et al. Monoclonal Antibody Blockade of the Human Eag1 Potassium Channel Function Exerts Antitumor Activity. *Cancer Res.* **2007**, *67*, 7343–7349. [[CrossRef](#)] [[PubMed](#)]
14. Mello de Queiroz, F.; Suarez-Kurtz, G.; Stühmer, W.; Pardo, L.A. Ether à Go-Go Potassium Channel Expression in Soft Tissue Sarcoma Patients. *Mol. Cancer* **2006**, *5*, 42. [[CrossRef](#)] [[PubMed](#)]
15. Asher, V.; Khan, R.; Warren, A.; Shaw, R.; Schalkwyk, G.V.; Bali, A.; Sowter, H.M. The Eag Potassium Channel as a New Prognostic Marker in Ovarian Cancer. *Diagn. Pathol.* **2010**, *5*, 78. [[CrossRef](#)] [[PubMed](#)]
16. Martínez, R.; Stühmer, W.; Martin, S.; Schell, J.; Reichmann, A.; Rohde, V.; Pardo, L. Analysis of the Expression of Kv10.1 Potassium Channel in Patients with Brain Metastases and Glioblastoma Multiforme: Impact on Survival. *BMC Cancer* **2015**, *15*, 839. [[CrossRef](#)]
17. Agarwal, J.R.; Griesinger, F.; Stühmer, W.; Pardo, L.A. The Potassium Channel Ether à Go-Go Is a Novel Prognostic Factor with Functional Relevance in Acute Myeloid Leukemia. *Mol. Cancer* **2010**, *9*, 18. [[CrossRef](#)]
18. Ding, X.-W.; Luo, H.; Jin, X.; Yan, J.; Ai, Y. Aberrant Expression of Eag1 Potassium Channels in Gastric Cancer Patients and Cell Lines. *Med. Oncol. Northwood Lond. Engl.* **2007**, *24*, 345–350. [[CrossRef](#)]
19. Menéndez, S.T.; Villaronga, M.A.; Rodrigo, J.P.; Alvarez-Teijeiro, S.; García-Carracedo, D.; Urduñigo, R.G.; Fraga, M.F.; Pardo, L.A.; Vilorio, C.G.; Suárez, C.; et al. Frequent Aberrant Expression of the Human Ether à Go-Go (HEAG1) Potassium Channel in Head and Neck Cancer: Pathobiological Mechanisms and Clinical Implications. *J. Mol. Med.* **2012**, *90*, 1173–1184. [[CrossRef](#)]
20. Ousingawatt, J.; Spitzner, M.; Puntheeranurak, S.; Terracciano, L.; Tornillo, L.; Bubendorf, L.; Kunzelmann, K.; Schreiber, R. Expression of Voltage-Gated Potassium Channels in Human and Mouse Colonic Carcinoma. *Clin. Cancer Res.* **2007**, *13*, 824–831. [[CrossRef](#)]
21. Toplak, Ž.; Hendrickx, L.A.; Abdelaziz, R.; Shi, X.; Peigneur, S.; Tomašič, T.; Tytgat, J.; Peterlin-Mašič, L.; Pardo, L.A. Overcoming Challenges of HERG Potassium Channel Liability through Rational Design: Eag1 Inhibitors for Cancer Treatment. *Med. Res. Rev.* **2022**, *42*, 183–226. [[CrossRef](#)] [[PubMed](#)]
22. Šterbuleac, D.; Maniu, C.L. An Antiarrhythmic Agent as a Promising Lead Compound for Targeting the HEAG1 Ion Channel in Cancer Therapy: Insights from Molecular Dynamics Simulations. *Chem. Biol. Drug Des.* **2016**, *88*, 683–689. [[CrossRef](#)]
23. Wang, W.; MacKinnon, R. Cryo-EM Structure of the Open Human Ether-à-Go-Go-Related K⁺ Channel HERG. *Cell* **2017**, *169*, 422–430.e10. [[CrossRef](#)]
24. Moreels, L.; Bhat, C.; Voráčová, M.; Peigneur, S.; Goovaerts, H.; Mäki-Lohiluoma, E.; Zahed, F.; Pardo, L.A.; Yli-Kauhaluoma, J.; Kiuru, P.; et al. Synthesis of Novel Purpurealidin Analogs and Evaluation of Their Effect on the Cancer-Relevant Potassium Channel KV10.1. *PLoS ONE* **2017**, *12*, e0188811. [[CrossRef](#)] [[PubMed](#)]
25. Gómez-Lagunas, F.; Carrillo, E.; Pardo, L.A.; Stühmer, W. Gating Modulation of the Tumor-Related Kv10.1 Channel by Mibefradil: Kv10.1 Channel Modulation by Mibefradil. *J. Cell. Physiol.* **2017**, *232*, 2019–2032. [[CrossRef](#)] [[PubMed](#)]
26. Toplak, Ž.; Hendrickx, L.A.; Gubič, Š.; Možina, Š.; Žegura, B.; Štern, A.; Novak, M.; Shi, X.; Peigneur, S.; Tytgat, J.; et al. 3D Pharmacophore-Based Discovery of Novel Kv10.1 Inhibitors with Antiproliferative Activity. *Cancers* **2021**, *13*, 1244. [[CrossRef](#)] [[PubMed](#)]
27. Gómez-Varela, D.; Contreras-Jurado, C.; Furini, S.; García-Ferreiro, R.; Stühmer, W.; Pardo, L.A. Different Relevance of Inactivation and F468 Residue in the Mechanisms of HEag1 Channel Blockage by Astemizole, Imipramine and Dofetilide. *FEBS Lett.* **2006**, *580*, 5059–5066. [[CrossRef](#)] [[PubMed](#)]
28. García-Ferreiro, R.E.; Kerschensteiner, D.; Major, F.; Monje, F.; Stühmer, W.; Pardo, L.A. Mechanism of Block of HEag1 K⁺ Channels by Imipramine and Astemizole. *J. Gen. Physiol.* **2004**, *124*, 301–317. [[CrossRef](#)]
29. Demovšek, J.; Zajec, Ž.; Durcik, M.; Mašič, L.P.; Gobec, M.; Zidar, N.; Tomašič, T. Structure-Activity Relationships of Benzothiazole-Based Hsp90 C-Terminal-Domain Inhibitors. *Pharmaceutics* **2021**, *13*, 1283. [[CrossRef](#)]
30. Surry, D.S.; Buchwald, S.L. Dialkylbiaryl Phosphines in Pd-Catalyzed Amination: A User's Guide. *Chem. Sci.* **2010**, *2*, 27–50. [[CrossRef](#)]
31. Boydston, A.J.; Rice, J.D.; Sanderson, M.D.; Dykhno, O.L.; Bielawski, C.W. Synthesis and Study of Bidentate Benzimidazolylidene—Group 10 Metal Complexes and Related Main-Chain Organometallic Polymers. *Organometallics* **2006**, *25*, 6087–6098. [[CrossRef](#)]
32. Arcangeli, A. Expression and Role of HERG Channels in Cancer Cells. *Novartis Found. Symp.* **2005**, *266*, 225–232. [[PubMed](#)]
33. Wang, H.; Zhang, Y.; Cao, L.; Han, H.; Wang, J.; Yang, B.; Nattel, S.; Wang, Z. HERG K⁺ Channel, a Regulator of Tumor Cell Apoptosis and Proliferation. *Cancer Res.* **2002**, *62*, 4843–4848. [[PubMed](#)]